PHYSICAL REVIEW D VOLUME 18, NUMBER 7 1 OCTOBER 1978

Constituent transverse-momentum fluctuations and the hard-scattering expansion

W. E. Caswell,* R. R. Horgan, and S. J. Brodsky
Stanford Linear Accelerator Center, Stanford University, Stanford, California 94305
(Received 19 April 1978)

We show that the cross section for large-transverse-momentum reactions $A + B \to C + X$ can be expanded in terms of a sum of incoherent hard-scattering reactions where groups of interacting constituents have small transverse momenta relative to A, B, or C. The effects of large-transverse momentum of the constituents cannot be represented in terms of simple convolution integrals, but are correctly incorporated in terms of a sum of subprocesses which, in physical processes, usually correspond to nonleading terms. This hard-scattering expansion yields a series in inverse powers of $\vec{p}_T{}^2$ in the case of ϕ^3 field theory or the constituent-interchange model, and a series in inverse powers of $\log(\log p_T^2)$ in the case of asymptotically free field theories.

I. INTRODUCTION

The study of high-transverse-momentum products in proton-proton collisions is very important to our understanding of the structure and dynamics of hadrons.[1,2] The most successful models[3-5] separate the scattering into two steps, first the emission of a constituent from each proton and then the large-angle scattering of these constituents as a subprocess. In addition to single-particle inclusive processes at high transverse momenta, these hard-scattering models predict jet processes in which the products of the hard subprocess each fragment (or decay) into several particles which amongst themselves have small relative transverse momenta but which, taken together, have a large transverse momentum relative to the incoming beam direction. The study of such jets gives new information on the properties of the hard-scattering process. The correlations between single particles[6,7] or jets[8] on one side and jets on the other side is particularly sensitive to the transverse momentum of the subprocess relative to the collision axis. Anomalously large transverse momenta have been observed for lepton pairs in the Drell-Yan production of $\mu^+\mu^-$ (Ref. 9) and this suggests that the transverse momentum of the quark constituents should be included in the description of such processes. We shall call the constituent transverse momentum, (transverse) fluctuations.

Constituent fluctuations have generally been neglected in calculations because they have been assumed to be much smaller than the relevant kinematic parameters of the high-p_T process (total energy, detected transverse momentum, invariant masses). Their size was taken to be of the order of the typical meson transverse momentum in hadronic processes, a few hundred MeV, but it has been noted that the transverse momenta of the constituents which fragment along the collision axis could be as large as 1 GeV.[10] This remark implies a substantial spread in transverse momentum of the constituents within the incident particles themselves.

It is evident that the effect of constituent fluctuations merits detailed study especially in the light of striking claims that such fluctuations can strongly affect the predictions for the cross section[4,11,12] and the power-law behavior of high-transverse-momentum processes.[4,6]

Parton models for large-transverse-momentum processes $A+B\to C+X$ are generally based on the probablistic expression[1] corresponding to Fig. 1(a)

$$E\frac{d^3\sigma}{dp^3}(A+B\to C+X)=\sum_{ab\to cd}\int_0^1 dx_a G_{a/A}(x_a)\int_0^1 dx_b G_{b/B}(x_b)\int_0^1 \frac{dx_C}{x_C{}^2}G_{C/c}(x_C)\delta(\hat{s}+\hat{t}+\hat{u})\frac{\hat{s}}{\pi}\frac{d\sigma}{d\hat{t}}(a+b\to c+d)\,, \tag{1.1}$$

where the $G(x)$ are the probability distributions in the (light-cone) variable x, and $\hat{s}=x_a x_b s$, $\hat{t}=(x_a/x_C)t$, $\hat{u}=(x_b/x_C)u$ are the Mandelstam variables of the subprocess, which is effectively on shell. In general there is an incoherent sum over the contributing hard-scattering reactions $a+b\to c+d$. Equation (1.1) is normally derived in model field theories after making a rather long list of approxi-

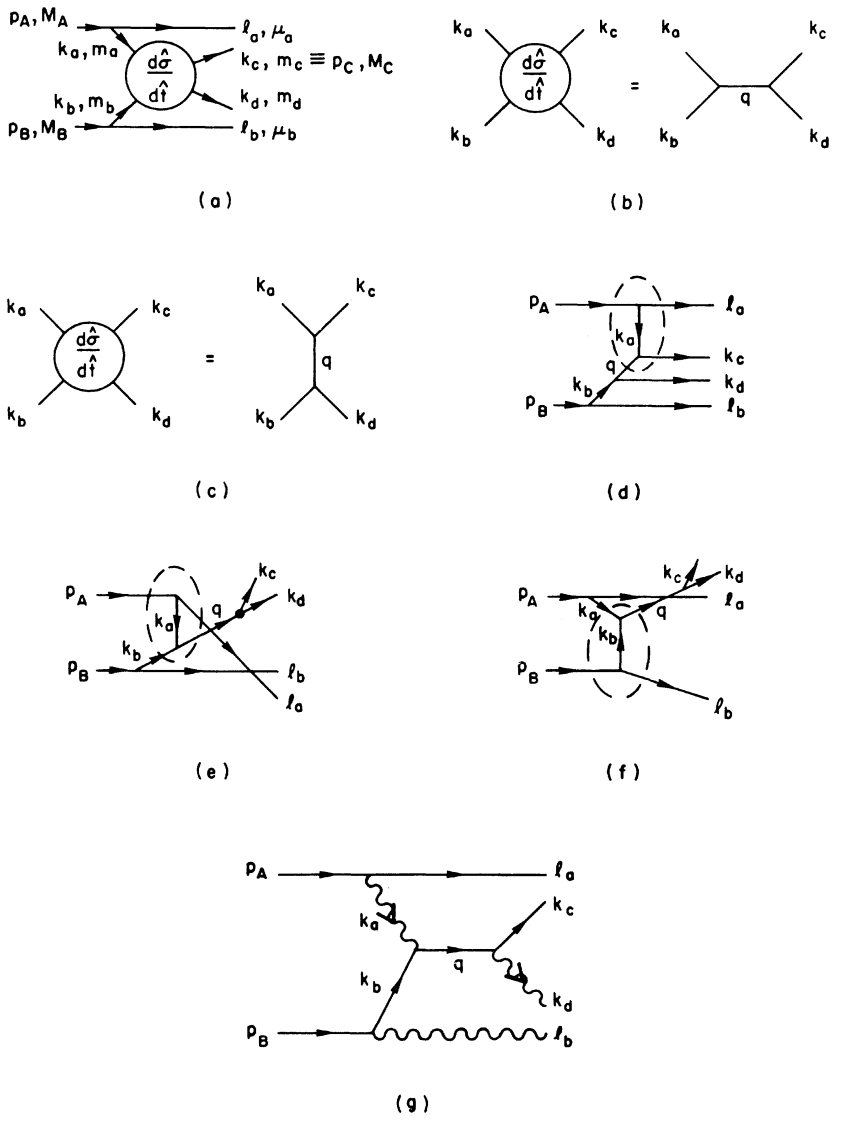

FIG. 1. Contributions to the hard-scattering process: (a) Example of hard-scattering subprocess and definition of momenta. (b) $\hat{s}$-pole subprocess in ϕ^3 field theory. (c) $\hat{t}$-pole subprocess in ϕ^3 field theory. (d) The subprocess other than that of Fig. 1(c) contributing in leading order to the $\hat{t}$-pole hard-scattering expansion in ϕ^3 field theory. (e) and (f): The two subprocesses other than that of Fig. 1(b) contributing in leading order to the $\hat{s}$-pole hard-scattering expansion in ϕ^3 field theory. (g) QCD (or QED) analog of the ϕ^3 field theory $\hat{s}$-pole scattering process.

mations. In Sec. II we enumerate some approximations and illustrate their accuracy quantitatively. In fact we show that if all leading subprocesses are included in the sum in Eq. (1.1) then Eq. (1.1) gives the exact large-p_T cross section to leading order.

It is often assumed that Eq. (1.1) can be immediately generalized to include transverse fluctuations by using simple convolutions of $d\sigma/d\hat{t}$ (taking $\hat{s}=x_a x_b s - 2\vec{k}_T^a \cdot \vec{k}_T^b$, etc.) with probability distributions $G_{a/A}(x_a, \vec{k}_{Ta})$, $G_{b/B}(x_b, \vec{k}_{Tb})$, and $G_{C/c}(x_C, \vec{k}_{TC})$. Although this procedure may have heuristic value for small transverse fluctuations, it becomes increasingly misleading at large k_T. The difficulties are related to the following considerations.

(1) The interacting partons a and b are in general off shell and spacelike, we can write

$$k_a^2 = -\left[\frac{\vec{k}_{Ta}^{\,2} + m^2(x_a)}{1-x_a}\right]$$

since p_A and $p_A - k_a$ are effectively on the mass

shell. [The quantity $m^2(x_a)$ is a linear combination of particle masses squared.] Thus for large k_{Ta} and/or $x_a \to 1$ the subprocess $d\sigma/d\hat{t}(a+b \to c+d)$ must be evaluated far off shell. In the case of (massless) gluon-exchange contributions in quantum chromodynamics (QCD) calculations, this fact ensures that the gluon pole at $\hat{t}=0$ never occurs in the physical region. This crucial effect was neglected in the early calculations of Ref. 6 where artificial cutoffs were needed to ensure finite results for a gluon-exchange model.

(2) Because of the off-shell nature of the interacting particles, the gauge invariance of subprocesses involving gauge fields cannot be maintained in simple hard-scattering models. Further, it is clear that the probabilistic interpretation of the parton models fails; from the perspective of time-ordered perturbation theory, nonclassical time-orderings of the interactions must be included when the intermediate states are far off the energy shell (large k_T or $x \to 1$).

(3) In general there are other processes such as $a+b \to c+d+e$ where three (or more) systems (jets or clusters) are produced with large transverse momentum and where the invariant mass of any pair grows with p_T. The contributions from such subprocesses give additional terms in the summation [Eq. (1.1)] and represent coherence corrections from $a+b \to c+d$ in the large-k_T region. In softened field theories, such contributions are nonleading by powers of p_T. In renormalizable theories, the relative suppression is only logarithmic. We discuss this in detail in Secs. II and III.

(4) The heuristic approach to transverse-momentum fluctuations leads to confusion concerning the identification of subprocesses. For example, consider the contribution to large-p_T quark-jet production in pp collisions arising from $qq \to qq$ shown in Fig. 2(a). The radiated gluon in the figure is one source of k_T fluctuations for the interacting quarks. When such fluctuations are large (of order p_T) this contribution to the Feynman diagram is better represented by Fig. 2(b) which can be identified with the parton-model subprocess $qg \to qg$. As another example consider the contribution to a high-p_T meson-baryon reaction shown in Fig. 2(c). From one point of view, this is simply a high-p_T $q\bar{q} \to q\bar{q}$ scattering reaction where the $\bar{q}$ already has a substantial transverse-momentum fluctuation in the direction of the detector. However, because of the fact that the interacting $\bar{q}$ at large $k_T \propto p_T$ is far off shell (spacelike), the mass of the $q\bar{q}$ system in the final state can be very small. In fact in the case of $MB \to M'X$, i.e., a high-p_T single-meson trigger, the $q\bar{q}$ system can be identified with the trigger particle. [This is actually a favored configuration since there is no suppression factor (typically of order 10^{-2}) from quark fragmentation $q \to M'$.] Thus from this point of view, the hard-scattering subprocess can be considered as $Mq \to M'q'$ where the interacting constituents have negligible k_T fluctuations. Thus because of the lack of precision in the definition of hard-scattering models, two seemingly dissimilar models are actually equivalent.

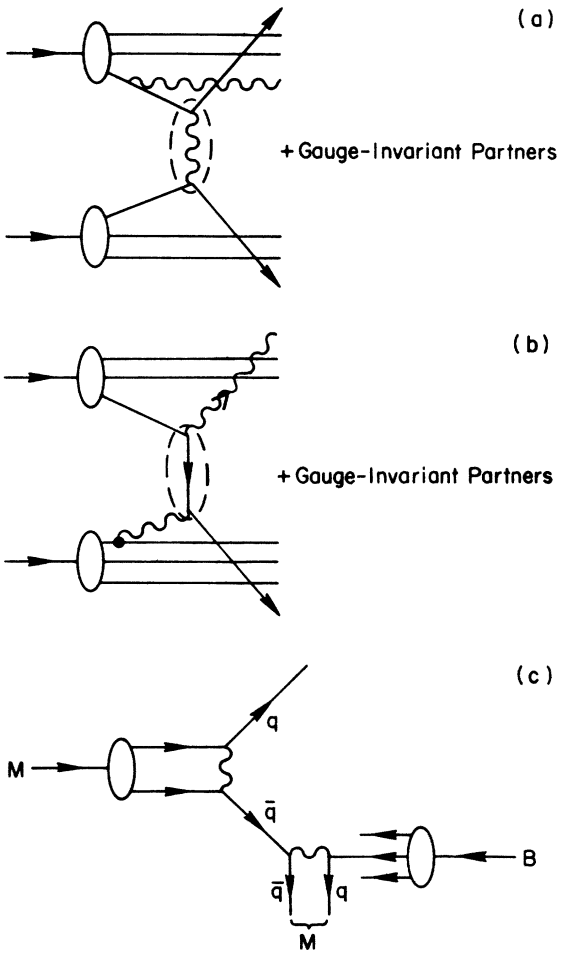

FIG. 2. (a) quark+quark→quark+quark (gluon brehmsstrahlung contribution). (b) quark+gluon→ gluon +quark. (c) The rearrangement of the $q\bar{q} \to q\bar{q}$ subscatter in $M+B$ scattering to show the contributing subprocess $M+q \to M+q$.

Although the $q\bar{q} \to q\bar{q}$ subprocess has canonical p_T^{-4} scaling in a renormalizable theory such as QCD Born diagrams, one easily finds that the subprocess $Mq \to Mq'$ gives a p_T^{-8} contribution to inclusive reactions. In fact, the subprocess[3]

$$\frac{d\sigma}{d\hat{t}}(Mq \to M'q') = \frac{C}{\hat{s}\hat{u}^3}$$

(which is part of the constituent-interchange model) is consistent with the scaling behavior and angular dependence of the subprocess extracted phenomenologically from Fermilab and CERN ISR $pp \to MX$ data below $p_T = 8$ GeV assuming no k_T fluctuations.[3]

(5) It is unnatural to consider arbitarily large k_T fluctuations (i.e., $k_T \propto p_T$) as arising from an intrinsic parton-momentum distribution with a hadron. In order for such fluctuations to occur there must be an internal hard-scattering processes (obtained, for example, from the iteration of the Bethe-Salpeter kernel), where the other constituents or gluons take up the recoil. Thus if we again consider Fig. 2 from the standpoint of (off-shell) $\bar{q}q \to \bar{q}q$ scattering, the production of the high-p_T systems cannot be localized within a single hard-scattering subprocess.

It is clear that as long as one considers small transverse-momentum fluctuations satisfying

$$\frac{\vec{k}_{Ta}^{\,2}}{1-x_a} \ll p_T^{\,2}, \quad \frac{\vec{k}_{Tq}^{\,2}}{1-x_b} \ll p_T^{\,2},$$

the ambiguities and problems discussed above should give only nonleading corrections. However, for $k_T^{\,2} \sim O(p_T^{\,2}(1-x))$, the parton hard-scattering model becomes ill defined.

The only reliable solution to the above list of ambiguities resulting from high-transverse-momentum fluctuations is to carefully follow the guide of exact Feynman-diagram calculations. Despite such complexities we have found in some model field theories that one can still define with some precision and numerical accuracy a hard-scattering expansion in which the transverse-momentum fluctuations are implicitly included. In these model calculations, we have verified that the complete Feynman-diagram contribution can be accurately expressed at large p_T as a *sum* over distinguishable on-shell, low-transverse-fluctuation subprocesses $ab \to cd$, where each of the interacting systems a, b, c, d are in general *multiparticle* systems. The scaling behavior in p_T of each contribution can then be determined from the total number of active particles in the subprocess, using dimensional-counting rules.[18] Further, the contribution from each of the subprocesses is well approximated by ignoring transverse fluctuations.

In the context of the hard-scattering models[1,3,13] we have examined the effect of constituent fluctuations on the cross section for detecting a particle at large transverse momentum in proton-proton collisions. All our calculations are for the cases where the detected particle is emitted at 90° to the collision axis, although this is not crucial. The fluctuation-independent distribution functions for the emission of a quark from a proton are taken from the SLAC data on lepton-proton scattering,[14] and the transverse fluctuations are included by multiplying these functions by various normalized x-dependent distributions.

We have paid particular attention to the effects of some common approximations to the kinematics and dynamics of such processes in both physical and model processes. In Sec. II we consider an exact model ϕ^3 field-theory analog of relevant processes and we use it as a theoretical laboratory to discuss and illuminate the effects of approximations and their pitfalls. We contrast subprocesses which are respectively described by $\hat{s}$- and $\hat{t}$-channel poles. The transverse fluctuations have an effect which can be directly interpreted in terms of a hard-scattering expansion of the full cross section discussed in Sec. IIC. Each term conforms to the kinematic restrictions of the parton model in which the constituents have limited transverse momentum; hence the necessity for grafting transverse fluctuations onto the parton model in some approximate way is obviated.

In Sec. IV we consider several physically important subprocesses and discuss the effect of transverse fluctuations in the context of the approach developed in Secs. II and III. The single-lepton spectrum from the Drell-Yan process as a function of transverse momentum derived from a rapidly falling distribution is found to be very nearly independent of the effects of such constituent fluctuations in agreement with the discussion in Secs. II and III. Other competing subprocesses for lepton-pair and single-lepton production are listed. One model in particular is discussed[15] which may be interpreted as the origin of a dominant contribution to the transverse-momentum distribution of antiquarks in the proton at intermediate values of k_T and which explains the experimentally observed transverse-momentum distribution of μ pairs as a function of their invariant mass. We find that at high transverse momentum the single-lepton spectrum predicted by this process agrees with that predicted by the naive ($q\bar{q} \to \mu\bar{\mu}$) calculation. Prompt meson production in the constituent-interchange model (CIM) is briefly considered, and we discuss the quark-scattering subprocess for quark-jet production. In the latter case the errors of an on-shell approach are illustrated and the effects of quark transverse fluctuations are interpreted in terms of new subprocesses contributing to quark-jet production at high p_T.

In Sec. V we present our conclusions and suggest a general method for analyzing contributions to high-momentum-transfer processes involving bound states which is applicable to renormalizable and super-renormalizable theories.

II. STUDY OF AN EXACT MODEL: ϕ^3 THEORY

In order to study the various approximations usually made in large-transverse-momentum calculations, we shall study in detail the behavior of the Born-diagram structure of ϕ^3 field theory which we can evaluate exactly. The principal features of the calculation mimic the phenomenological features of most hard-scattering models, including the p_T^{-8} behavior of the $pp \to \pi X$ data at fixed $x_T = 2p_T/\sqrt{s}$ and $\theta_{\text{c.m.}}$.

A. Kinematics

In ϕ^3 field theory we consider scattering processes of the type depicted in Fig. 1(a) with the particles labeled by their four-momenta. All kinematic variables are defined in the usual manner[16] and those referring to the hard-scattering subprocess $(k_a, k_b) \to (k_c, k_d)$ are $\hat{s}$, $\hat{t}$, and $\hat{u}$. We separately discuss the two cases shown in Fig. 1(b) and Fig. 1(c) in which the subprocess is represented by an $\hat{s}$-channel pole and a $\hat{t}$-channel exchange, respectively. The differential cross section may be written as[16]

$$d\sigma = g^4 \left| \frac{1}{k_a^2 - \mu_a^2} M \right|^2 \frac{(2\pi)^4}{\sqrt{\Delta}} \delta^4(p_A + p_B - l_a - l_b - k_c - k_d) \times \prod_f \frac{d^4 p_f}{(2\pi)^3} \delta^+(p_f^2 - m_f^2), \tag{2.1}$$

where

$$\Delta \equiv \Delta(s, m_A^2, m_B^2) = [s - (m_A + m_B)^2][s - (m_A - m_B)^2],$$

g is the vertex coupling constant, and

$$M = \begin{cases} g^2[(k_a + k_b)^2 - m^2]^{-1} & \text{for } \hat{s}\text{-pole case} \\ g^2[(k_a - k_c)^2 - m^2]^{-1} & \text{for } \hat{t}\text{-pole case}. \end{cases}$$

In the following we consider any collinear frame where the incident particles define the $\hat{z}$ direction. Momenta are denoted by $k^\mu = (k^0, \vec{k}, k^3)$. We analyze the cross section (2.1) in terms of light-cone variables (16) defined by

$$x_a = (k_a^0 + k_a^3)/(p_A^0 + p_A^3), \quad x_b = (k_b^0 - k_b^3)/(p_B^0 - p_B^3).$$

[Unless otherwise stated all formulas that are given for (a, A) alone are valid for $(a, A) \to (b, B)$.] Then

$$\int d^4 l_a \delta^{(+)}(l_a^2 - \mu_a^2) = \int d^2\vec{k}_a \int_0^1 \frac{dx_a}{2(1 - x_a)}. \tag{2.2}$$

The parton four-momentum k_a^μ is determined by momentum conservation and is not on the mass shell but satisfies

$$k_a^2 = x_a \left(M_A^2 - \frac{\vec{k}_a^2 + \mu_a^2}{(1 - x_a)} - \frac{\vec{k}_a^2}{x_a} \right), \tag{2.3}$$

where we always take $M_A < \mu_a + m_a$. We define the vertex distribution function

$$G_{a/A}(x_a, \vec{k}_a) = \frac{g^2}{2(2\pi)^3} \frac{x_a(1 - x_a)}{[\vec{k}_a^2 + (1 - x_a)(m_a^2 - x_a M_A^2) + x_a \mu_a^2]^2}. \tag{2.4}$$

The subprocess invariant cross section is given by

$$\frac{d\sigma}{d\hat{t}} = \frac{1}{16\pi} \frac{1}{\hat{\Delta}} M^2,$$

where

$$\hat{\Delta} \equiv \Delta(\hat{s}, m_a, m_b) = [\hat{s} - (m_a + m_b)^2][\hat{s} - (m_a - m_b)^2].$$

Using (2.2) and (2.4) we can cast (2.1) into the form of an invariant differential cross section for detecting particle p [$\equiv k_c$, see Fig. 1(a)]

$$p^0 \frac{d^3\sigma}{dp^3} = \frac{1}{\pi} \int dx_a d\vec{k}_a dx_b d\vec{k}_b G_{a/A}(x_a, \vec{k}_a) G_{b/B}(x_b, \vec{k}_b) \times \frac{1}{x_a x_b} \frac{\hat{\Delta}}{\sqrt{\Delta}} \frac{d\sigma}{dt} \delta(\hat{s} + \hat{t} + \hat{u} - k_a^2 - k_b^2 - m_c^2 - m_d^2). \tag{2.5}$$

The function $G_{a/A}(x_a, \vec{k}_a)$ was defined in such a way that the form of (2.5) has a simple parton-model interpretation. $G_{a/A}(x_a, \vec{k}_a) dx_a d\vec{k}_a$ is interpreted as the number of partons a emitted by particle A with longitudinal momentum fraction between x_a and $x_a + dx_a$ (in the high-energy limit or in the infinite-momentum frame) and with transverse momentum between $\vec{k}_a$ and $\vec{k}_a + d\vec{k}_a$. The partons k_a and k_b then scatter in an independent subprocess except that the particle flux is defined by $x_a x_b s$ and not $\hat{s}$. However, even though such an interpretation of (2.5) is seductive in its simplicity, we must emphasize that (2.5) is an exact representation of the process shown in Fig. 1(a) when interpreted as a Feynman diagram, in which case the transverse-momentum distribution of the partons is predicted and is given by (2.4). The kinematic region over which (2.5) is integrated is determined by solving the following constraints[17]:

$$\begin{aligned} &0 \le x_a, x_b \le 1, \\ &\hat{s} \ge (m_c + m_d)^2, \\ &P^2 = \left(\frac{\bar{s}\bar{t}\,\bar{u} - k_a^2 \bar{u}^2 - k_b^2 \bar{t}^2}{\Delta(\hat{s}, k_a^2, k_b^2)} - M_c^2 \right) \ge 0, \end{aligned} \tag{2.6}$$

where

$$\bar{s} = \hat{s} - k_a^2 - k_b^2, \quad \bar{t} = \hat{t} - k_a^2 - m_c^2,$$

$$\bar{u} = \hat{u} - k_b^2 - m_c^2.$$

P is the transverse momentum of k_c or k_d in the subprocess center-of-mass frame. The δ function in (2.5) must also be solved to yield a relation be-

tween the integration variables.

In Sec. II B we will compare the exact calculation (2.5) with various approximations. From the form of (2.5) it is easy to infer the effective power-law behavior of the invariant cross sections for $x_T \sim 1$ or $x_T \sim 0$

$$p^0 \frac{d^3\sigma}{dp^3} \to \frac{g^4}{\overline{m}^4} g^4 \frac{x_T{}^4(1-x_T)^3}{p_T{}^8} f(\theta_{\text{c.m.}}), \tag{2.7}$$

where $x_T = 2p_T/\sqrt{s}$, and $g^2/\overline{m}^2$ results from the integration of $G(x, \vec{k})$ over $\vec{k}$.

In order to estimate which kinematic regions of the integral (2.5) yield the most important contributions to the cross section at large transverse momentum we must isolate all important hard-scattering subprocesses. Following the counting rules[18] (which follow from dimensional analysis), each subprocess at fixed x_T behaves like $1/(p_T{}^2)^N$ where $N = \lambda \times$ (no. participating particles -2) where $\lambda = 2$ for the ϕ^3 theory and $\lambda = 1$ for the renormalizable theory. The power F of $(1-x_T)$ is given by $[2 \times (\text{number of spectator particles})] - 1$. In Fig. 1(a)–1(c) the subprocess selected for illustration is the one which leads to the conventional parton-model interpretation discussed earlier where k_c recoils against k_d. However, in both cases 1(b) and 1(c), subprocesses other than those illustrated are equally important and these are shown ringed by dotted lines in Fig. 1(d) and Figs. 1(c) and 1(f), respectively. These extra subprocesses all give contributions which behave like $p_T{}^{-8}$ for fixed x_T. The high transverse momentum generated by the process of Fig. 1(d) is produced by k_c recoiling against l_a. In this subprocess k_a is the t-channel exchange particle and hence $k_a{}^2$ must be assigned its exact off-shell spacelike value of order $-\vec{k}_T{}^2/(1-x_a)$ given by (2.3). [We ought not to fix $k_a{}^2 = m_a{}^2$ as an approximation any more than we would put the exchanged particle in the original $\hat{t}$-channel subprocess (Fig. 1c) on shell. Indeed, if we did the latter the calculation would lose all semblance of credibility.] From Eq. (2.3) the off-shell value of $k_a{}^2$ depends (apart from masses) on the value of x_a and $\vec{k}_a{}^2$ which, for the subprocess of Fig. 1(d), is of the order of the $p_T{}^2$ of the trigger particle k_c. Consequently, the isolation of this subprocess explicitly shows the contribution that the transverse momentum $\vec{k}_a$ of the parton (relative to its parent $\vec{p}_A$) makes to the total large-p_T scattering cross section.

The process of Fig. 1(e) contributes to the $p_T{}^{-8}$ behavior of the cross section at fixed x_T and the high transverse momentum is produced by q recoiling against l_a. The trigger particle k_c is then produced by fragmentation (or decay) of q as one member of the low mass pair (k_c, k_d). As emphasized above, $k_a{}^2$ should be assigned its correct off-shell spacelike value in order for this subprocess to be correctly included.

In the language used so far the effect of transverse-momentum fluctuations of a given parton is determined by analyzing all possible hard-scattering subprocesses in which that parton carries the large-p_T momentum. Counting rules then tell us whether such processes contribute in the leading order or not. This procedure treats all kinematic regions democratically and never begins by assuming that transverse-momentum fluctuations may be ignored as an approximation when calculating leading-order effects. Thus the production of a large p_T particle can always be identified with one or more explicit hard-scattering subprocesses. Using this enumeration, one need never refer to parton-model wave functions with large-transverse-momentum fluctuations.

In the phenomenological parton-model picture which is often used as an approximation the fundamental process is defined to be given by Fig. 1(a) and the parton transverse-momentum distributions (2.4) are not necessarily determined by the internal consistency of the model. The integral expression for the invariant cross section (2.5) is then used with various approximations to the kinematics in order to predict the large-p_T behavior of the process. The fact that this prescription does not explicitly exhibit the democracy of the Feynamn-diagram approach discussed earlier does not detract from a given model which might be validated on physical grounds. However, such an approach may in some cases obscure the effects that a given approximation has on the final result. In this context a common error is to believe that the parton transverse-momentum fluctuations may always be included by convoluting the transverse-momentum distribution of the parton with the cross section calculated without fluctuations. Clearly the analysis discussed earlier cannot be interpreted in this way and a detailed inspection of (2.5) confirms that the integral cannot be rendered into the form of a convolution.

In the next subsection we discuss the effects of various common approximations to the integral (2.5), especially with regard to the breakdown of the full processes into the relevant subprocesses as described in this section. In order to compare later to the often made parton-model assumption (i.e., simple impulse approximations) we introduce an on-shell parametrization for the partons k_a and k_b. We define

$$\vec{k}_a^{\,\mu} = ([\vec{k}_a{}^2 + (x_a p_A{}^3)^2 + m^2]^{1/2}, \vec{k}_a, x_a p_A{}^3), \tag{2.8}$$

where x_a is the Feynman longitudinal-momentum fraction. This leads to a purely *ad hoc* modification of the integral (2.5) which is not kinematical-

ly consistent since it puts k_a and k_b on the mass-shell whereas we have already seen that momentum conservation requires $k_a^2 - m_a^2$ to be space-like. The largest error occurs when k_a^2 is farthest off shell which from (2.3) can be seen to be for large $\vec{k}_a^2$ or $x_a \to 1$. We will discuss the effects of putting the partons on mass shell for various large-p_T proton-proton processes in Sec. IV.

B. Effects of approximations

The kinematic constraints which determine the region of integration in (2.5) are given in (2.6). Other equivalent constraints may be substituted for those in (2.6) in terms of the external process variables s,t,u. However, in a calculation which approximates the kinematics there can be a mismatch between different sets of constraints and some may allow a region of integration to contribute which would be forbidden in an exact calculation (e.g., reaching a pole). As an example consider the process for which the detected particle is at 90° in the center-of-mass of the incident particles. In this case the δ function in (2.5) may be written, to leading order in s and ignoring masses, as

$$\delta(s+t+u-k_a^2-k_b^2)=\delta\left(x_a x_b s - p_T\sqrt{s}\,(x_a+x_b)+p_T^2 - \vec{k}_d^{\,2}+\frac{x_a\vec{k}_a^{\,2}}{(1-x_a)}+\frac{x_b\vec{k}_b^{\,2}}{(1-x_b)}\right), \tag{2.9}$$

where

$$\vec{k}_d=\vec{p}_T-\vec{k}_a-\vec{k}_b\,.$$

For $\vec{k}_a^{\,2}$ and $\vec{k}_b^{\,2}$ small this gives the usual solution

$$x_b=\frac{x_a p_T/\sqrt{s}}{x_a-p_T/\sqrt{s}}\,,$$

which, in conjunction with the falloff $(1-x)^N$ of the distribution functions $g(x,k)$, determines the major contribution to the integral (2.5) to be for x_a, $x_b \simeq 2p_T/\sqrt{s}$. For the t-exchange subprocess the pole would be reached for $\vec{k}_a \simeq \vec{p}_T$, $\vec{k}_b = 0$. Then

$$x_b=\left(\frac{x_a p_T}{\sqrt{s}}-\frac{p_T^2}{s(1-x_a)}\right)\Big/\left(x_a-\frac{p_T}{\sqrt{s}}\right)$$

which has solutions for $x_a \simeq 0$ and $x_b \simeq p_T\sqrt{s}$. However, for this particular region we find

$$\hat{s}=x_a x_b s-(\vec{k}_a-\vec{k}_b)^2+\frac{x_a k_a^{\,2}}{(1-x_a)}+\frac{x_b k_b^{\,2}}{(1-x_b)}\simeq -p_T^2$$

which is spacelike and hence unphysical since it cannot make two on-shell final-state particles. Generally the effect of the space-like momenta of the partons is to ensure that the main contribution to the integral is from the (well-understood) region where x_a, $x_b \simeq 2p_T/\sqrt{s}$. We should beware of any approximation which allows the integral to receive a contribution from physically forbidden regions. The relation between integration variables, because of the δ-function constraint, may also be altered by the approximations.

The exact expressions for the relevant kinematic variables are

$$s=(p_A+p_B)^2,\quad t=(p_A-p_C)^2,\quad u=(p_B-p_C)^2\,,$$

$$\hat{s}=(k_a+k_b)^2=x_a x_b s'+k_a^2+k_b^2-2\vec{k}_a\cdot\vec{k}_b+\frac{m_{a\perp}^{\,2}m_{b\perp}^{\,2}}{x_a x_b s'}\,,$$

$$\hat{t}=(k_a-k_c)^2=x_a t'+k_a^2+m_c^2+2\vec{k}_a\cdot\vec{p}_T+\frac{m_{a\perp}^{\,2}m_{c\perp}^{\,2}}{x_a t'}\,,$$

$$\hat{u}=(k_b-k_c)^2=x_b u'+k_b^2+m_c^2+2\vec{k}_b\cdot\vec{p}_T+\frac{m_{b\perp}^{\,2}m_{c\perp}^{\,2}}{x_b u'}\,,$$

$$p_T^2\equiv|\vec{k}_c|^2=\frac{s't'u'-M_A^{\,2}t'^2-M_B^{\,2}u'^2}{\Delta(s,M_A^{\,2},M_B^{\,2})}-M_c^2\,, \tag{2.10}$$

where

$$s'=p_A\cdot p_B+[(p_A\cdot p_B)^2-M_A^{\,2}M_B^{\,2}]^{1/2}\,,$$

$$t'=-p_A\cdot p_C-[(p_A\cdot p_C)^2-M_A^{\,2}M_C^{\,2}]^{1/2}\,,$$

$$u'=-p_B\cdot p_C-[(p_B\cdot p_C)^2-M_B^{\,2}M_C^{\,2}]^{1/2}\,,$$

$$m_{a\perp}^{\,2}=\vec{k}_a^{\,2}+k_a^2,\quad m_{b\perp}^{\,2}=\vec{k}_b^{\,2}+k_b^2,\quad m_{c\perp}^{\,2}=\vec{k}_c^{\,2}+m_c^2\,.$$

We have calculated the effects of several different approximations in the ϕ^3 theory for the two cases where the subprocess in Fig. 1(a) is taken to be an $\hat{s}$-channel pole or a $\hat{t}$-channel exchange pole. The results of this investigation are contained in Figs. 3–5. For the light-cone parametrization we have chosen six different approximations to the exact calculation which are

(1) No approximation—i.e., exact calculation.

(2) The matrix elements for the subprocess are simplified to be

$$M=\begin{cases} g^2(x_a x_b s-m^2)^{-1}, & \hat{s}\text{ pole}\\ g^2(x_a t-m^2)^{-1}, & \hat{t}\text{ pole}\,.\end{cases}$$

(3) The correct matrix elements are used but the transverse-momenta $\vec{k}_a$ and $\vec{k}_b$ are set equal to zero when calculating the effect of the δ-function constraint.

(4) As (3), but the simplified matrix elements defined in (2) are used; i.e., (4)=(3)+(2).

(5) The transverse momenta $\vec{k}_a$ and $\vec{k}_b$ are put equal to zero everywhere except in the parton distribution function which is trivially integrated over $\vec{k}_a$ and $\vec{k}_b$. The correct subprocess matrix elements are used.

(6) As (5), but the simplified matrix elements defined in (2) are used, i.e., (6)=(5)+(2). This

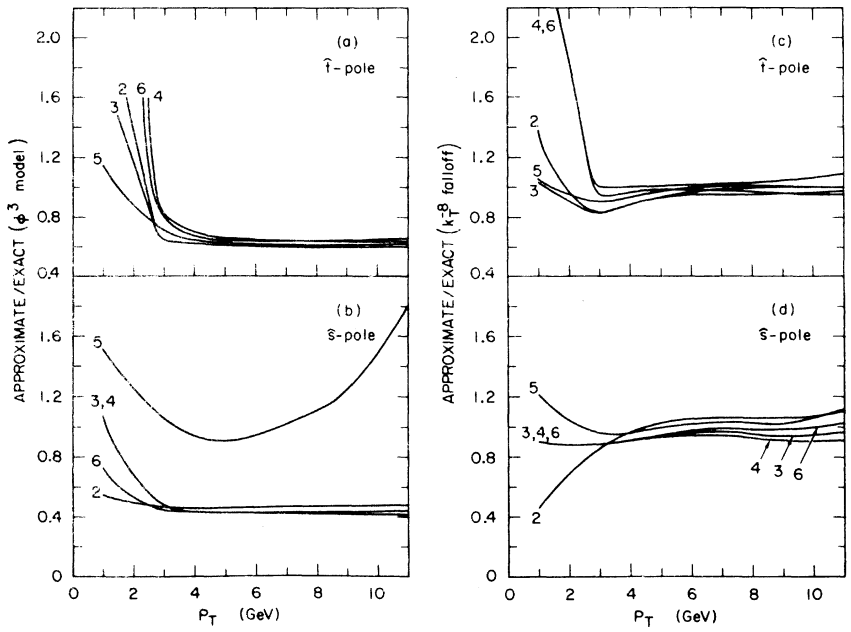

FIG. 3. The ratio of various approximate calculations to the exact calculation versus p_T ($s = 800$ GeV^2, $m = 1$ GeV) for high-p_T scattering in ϕ^3 field theory. The curves are labeled by the number of the particular approximation as given in Sec. II B. (a) $\hat{t}$-pole subprocess. (b) $\hat{s}$-pole subprocess. (c) $\hat{t}$-pole subprocess with (k_T^a, k_T^b) distribution replaced by $(k_T^2 + M(x^2))^{-4}$. The contribution of the subprocess of Fig. 1(d) is then suppressed. (d) As (c) but for $\hat{s}$-pole subprocess. The contributions of Fig. 1(e) and 1(f) are suppressed.

corresponds to the naive impulse approximation. The difference between (4) and (6) is the kinematic constraints (2.6) which are correctly included in (4).

The results of these approximations for the single-particle cross section at 90°, $s = 800$ GeV^2, with all particle masses set equal to 1 GeV are shown in Figs. 3(a) and 3(b) as a ratio to the exact calculation (1). For $s = 800$ GeV^2 we expect the range 3 GeV $\leq p_T \leq$ 9 GeV to best illustrate our ideas since the edge of phase space encroaches above $p_T = 9$ GeV, and below $p_T = 3$ GeV we should not expect to properly distinguish between leading and nonleading subprocess contributions. This is also the region in which parton-model calculations have been done to study high-transverse-momentum processes. From Fig. 3(a) in all cases the contribution from the $\hat{t}$-channel exchange graph is reduced in this range by a factor of about 1.5 because of the approximations made. In the $\hat{s}$-channel pole process from Fig. 3(b) for the same range of p_T the contribution is decreased by roughly a factor of 2 for all approximations except one. In all cases where a reduction occurs the reason for the decrease can be shown to be due to the elimination (by the pertinent approximation) of one of the extra subprocesses discussed in Sec. II A. For an example we consider approximation (2) in the $\hat{t}$-channel exchange process in which the simplified subprocess matrix element $M = g^2(x_a t - m^2)^{-1}$ is used. For the subprocess of Fig. 1(d) to contribute in leading order we require $\hat{t} = q^2 \simeq O(-m^2)$, $k_a^2 \simeq -p_T^2$ and the *exact* matrix element then behaves like $M_{ex} \simeq O(-g^2/2m^2)$. However, since $x_a \simeq p_T/\sqrt{s}$ and $t \simeq -p_T\sqrt{s}$ we find that the *simplified* matrix element behaves like $-g^2/p_T^2$ which consequently suppresses the contribution of the subprocess [1(d)] by a factor $\sim 4m^4/p_T^4$ with respect to its contribution in the exact calculation. From (2.9) we can see explicitly that in the region discussed above $\hat{t}$ can indeed have a small absolute value since the terms depending on $\vec{k}_a$ cancel the large negative contribution from $x_a t' + k_a^2$ when $k_a \simeq \vec{p}_T (\equiv \vec{k}_c)$ which is the case under consideration.

The result of approximation (5) may be similarly explained for this $\hat{t}$-pole process. Even when the integrand of (2.5) is being evaluated for large $\vec{k}_a$, the matrix element is approximated by its value at $\vec{k}_a = 0$. This is very similar to the case just discussed and because of the approximation the matrix element again behaves like $-g^2/p_T^2$ in a region where in the exact calculation it behaves like $-g^2/4m^2$. Consequently, the subprocess of Fig. 1(d) makes a negligible contribution. The effects of approximations (2) and (5) on the $\hat{s}$-channel pole process of Fig. 1(b) are analyzed in a manner

identical to that above where the processes of Figs. 1(e) and 1(f) become artificially suppressed.

It is interesting that the effect of approximation (3) suppresses the result in the $\hat{t}$-exchange case but not in the $\hat{s}$-pole case. In this approximation the δ-function constraint is calculated with $\vec{k}_a = \vec{k}_b = 0$. The constraint then becomes

$$x_a x_b s - (x_a + x_b) p_T \sqrt{s} \simeq 0 . \quad (2.11)$$

This overestimates x_a for a given x_b, and for $\vec{k}_a \simeq \vec{p}_T$, $\vec{k}_b = 0$ compared to the exact calculation in the same region, which requires

$$x_a x_b s - (x_a + x_b) p_T \sqrt{s} + 2{p_T}^2 - \frac{{p_T}^2}{1 - x_a} \simeq 0 . \quad (2.12)$$

Whichever of Eqs. (2.11) and (2.12) pertains, $\hat{s}$ is able to assume the small values [see (2.10)] (of order of the quark mass) required for the subprocesses of Fig. 1(e) and 1(f) to contribute. For the $\hat{s}$-pole process both x_a and x_b are calculated to be larger in the approximate situation [Eq. (2.11)] than in the exact calculation [Eq. (2.12)], but there is no suppression from the structure functions since $G(x) \sim x(1-x)$ and the product $G(x_a)G(x_b)$ assumes roughly equal values in the two cases [for $G(x) \sim (1-x)$ the approximate case would be suppressed]. For the $\hat{t}$-exchange process no values for x_a, $x_b (0 \leq x_a, x_b \leq 1)$ are compatible with (2.11) and $\hat{t} \sim O(-m^2)$ [see (2.10)] which is the requirement for the process shown in Fig. 1(d) to contribute in the approximate situation. $\hat{t}$ is forced to be $O({p_T}^2)$ and the result is therefore diminished because the contribution of the subprocess of Fig. 1(d) is suppressed by $O((m^2 {p_T}^2)^2)$. The remaining approximations are superpositions of those already discussed and so their effects are easily deduced.

In order to test the subprocess interpretation in a different way we modified the structure functions (2.4) so that the parton fluctuation distributions were

$$\bar{G}(x, \vec{k}) = G(x, \vec{k}) 3M^4(x) [\vec{k}^2 + M^2(x)]^{-2} ,$$

where $M(x)^2 = m^2(1 - x + x^2)$ and $G(x, \vec{k})$ is defined in (2.4) (equal-mass case). Because of the faster falloff in $\vec{k}$, only those subprocesses shown in Fig. 1(b) and 1(c) now contribute in the leading order. The effects of approximations (1)–(6) are shown for the $\hat{t}$-exchange pole and $\hat{s}$-channel pole processes in Figs. 3(c) and 3(d), respectively. As is expected there is no significant suppression in any of the cases [note the change of scale relative to Fig. 3(a) and 3(b)] since there are now no leading ${p_T}^{-8}$ subprocesses to be eliminated. This model is akin to usual models of physical processes where it is assumed that the parton transverse fluctuations fall off much faster than the transverse momentum in the central subprocess.

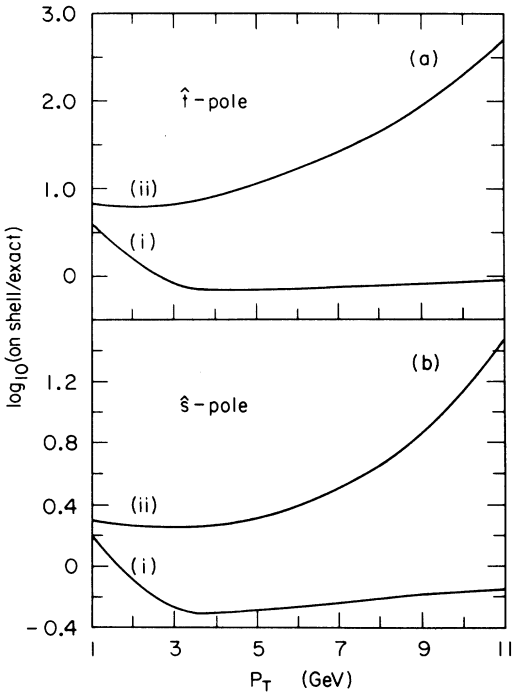

FIG. 4. Ratio of on-shell kinematics calculation to exact calculation versus p_T ($s = 800$ GeV^2, $m = 1$ GeV) for (i) no transverse fluctuations, (ii) $[{k_T}^2 + M(x)^2]^{-2}$ transverse-momentum distribution (logarithmic scale) (a) $\hat{t}$-pole subprocess. (b) $\hat{s}$-pole subprocess.

We have studied the effects of the on-shell parametrization (2.8) of the parton momenta in which the intermediate-state partons are on the mass shell ($k_a^2 = k_b^2 = m^2$) and the results obtained for $\hat{t}$-exchange and $\hat{s}$-channel pole processes, respectively, are compared in Figs. 4(a) and 4(b) with the equivalent calculations using the light-cone parametrization.

There are several relevant experimental quantities which we can study in the ϕ^3 model in order to estimate how accurately they can be predicted for the more complex physical processes. The effective-power analysis suggests that a good representation for the invariant cross section is

$$p^0 \frac{d^3\sigma}{dp^3} = \frac{A {x_T}^4 (1 - x_T)^3}{({p_T}^2 + m^2)^4} \simeq \frac{A(1 - x_T)^3}{({p_T}^2 + m^2)^2}$$

for a fixed energy. For $s = 800$ GeV^2 we fitted the form

$$\frac{1}{{x_T}^4} p^0 \frac{d^3\sigma}{dp^3} = \frac{A(1 - x_T)^F}{({p_T}^2 + m_{\text{eff}}^2)^N}$$

to the calculated invariant cross section over the range 3.5 GeV $\leq p_T \leq 8$ GeV ($0.25 \leq x_T \leq 0.55$, x_T

$= 2p_T/\sqrt{s}$). All masses were set equal to $m = 1$ GeV, and then the scale of the transverse fluctuations is of order 1 GeV^2. The fitted values of N and F were

$\hat{s}$-channel subprocess

$$N = 1.66 \pm 0.14, \quad F = 4.63 \pm 0.41,$$

$\hat{t}$-exchange subprocess

$$N = 1.75 \pm 0.16, \quad F = 4.63 \pm 0.49.$$

The errors quoted are the square roots of the diagonal covariance matrix elements for the linear least-squares fit to $\ln[p^0(d^3\sigma/dp^3)]$. The analytic value for N at $p_T{}^2 \gg m^2$ is $N = 2$, and for $x_T \to 1$ one predicts $F \to 3$. Deviations for N and F are expected because of the mass corrections and the limited range of x_T.

In general the other final-state particles do not lie in the plane defined by the incoming particles (k_A, k_B) and the detected particle $\vec{p}_a$. The three-momentum out of this plane is

$$\vec{p}_{\text{out}} = [\vec{p} \cdot (\hat{k}_A \times \hat{p}_a)]\hat{k}_A \times \hat{p}_a .$$

The average value of this variable is a measure of the scale of the transverse fluctuations of the intermediate constituents; $\langle \vec{p}_{\text{out}}{}^2 \rangle$ is calculated in the exact Feynman-graph calculation and is plotted as a function of p_T in Fig. 5 for both subprocesses discussed above. The fact that p_{out}, with $M_q = 1$ GeV is consistent with measured values indicates that the mass parameters which govern the magnitude of scale-breaking are set correctly in this model. It should be emphasized that even though the k_T fluctuations may give a small correction to the inclusive cross section, they still may contribute significantly to the physical values of quantities such as p_{out}.

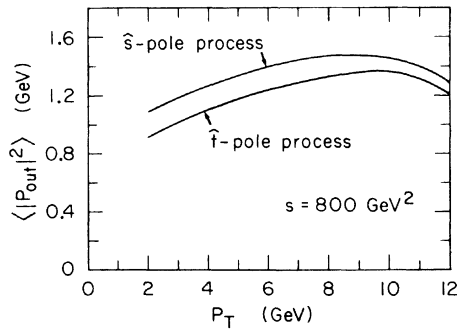

FIG. 5. $\langle |P_{\text{out}}|^2 \rangle$ distribution versus p_T ($s = 800$ GeV^2, $m = 1$ GeV) for (a) $\hat{t}$-pole subprocess (b) $\hat{s}$-pole subprocess.

C. Discussion

In order to understand the role of parton momentum we must consider the Feynman-graph interpretation of Fig. 1(a). The regions of integration from which the cross section receives its major power-law-behaved contributions must be analyzed by examining all the possible hard-scattering subprocesses. All leading-order subprocesses in p_T are *a priori* equally important to the integral. For a given leading subprocess the large transverse momentum is by definition generated by scattering within the subprocess and hence only particles internal to the subprocess carry large transverse momenta of order p_T. The initial constituents in the subscattering have only small k_T (i.e., much less than p_T) since otherwise they would constitute the high-p_T exchange particle of a different subprocess which has already been counted or which does not contribute in the leading order.

As an example consider the $\hat{t}$-channel pole which has two contributing subprocesses shown in Fig. 1(c) and 1(d). In Fig. 1(c), k_a and k_b are the incident constituents and q carries the large transverse momentum. In Fig. 1(d), p_A and q are the incident constituents and k_a carries the large transverse momentum. The latter subprocess isolates the contribution in which the erstwhile constituent k_a has large k_T. However, this particle is no longer interpreted as a constituent of the incident particle but as a participant created in the subprocess.

It is now clear that constituents can be defined consistently to have only small transverse momenta. This is, of course, necessary for the parton-model interpretation since it is required that the intermediate constituent state be close to the energy shell in old-fashioned perturbation theory,[19] which in turn demands that the constituents have small transverse momenta. The x distributions of each constituent differ with each choice of high-p_T subprocess. In our example of the subprocess in Fig. 1(c) we have, for both constituents, $G(x) \propto x(1-x)$. For the subprocess of Fig. 1(d) we have for constituent p_A, $G(x) = \delta(x-1)$ and for q, $G(x) \propto x(1-x)^3$. In this subprocess, q is a constituent from the three-body wave function of p_B, the other two constituents k_a and l_b have zero transverse momenta and are absorbed into a low-mass core. We thus recover the simple parton-model interpretation of the high-p_T scattering process where all constituents have small transverse momenta. We must sum over all possible subprocesses with the relevant constituent x distributions in order to obtain all the leading-order contributions of the exact approach. We refer to this summation as the hard-scattering expansion.

The results of the preceding analysis enable the following prescription to be formulated for calculationg all leading-order $p_T^{-n}f(x_T, \theta_{c.m.})$ contributions to the cross section for high-p_T inclusive processes. This prescription includes all effects which were hitherto known as parton transverse fluctuations but which are now sublated to new subprocesses.

(i) Respective constituent members (a,b) of the incident hadrons (A,B) are chosen. (These constituents may be elementary fields such as quarks or gluons or may be composites of these fields.) All remaining constituents of A and B are integrated into the respective cores $(A\bar{a}, B\bar{b})$ of these particles. These spectator systems have essentially fixed masses and have no transverse momentum.

(ii) The transverse momentum of the constituents is neglected and the x distributions $G_{a/A}(x_a)$ and $G_{b/B}(x_b)$ are determined either by analysis or by experiment (a more detailed discussion, including hadronic constituents can be found in Refs. 1, 3, and 18).

(iii) The high-p_T trigger particle C is produced in the subprocess $a+b\to c+\cdots$ as a fragment of the constituent c with fragmentation function $G_{C/c}(x_C)$. The differential cross section for the subprocess $d\sigma(\hat{s})/d\hat{t}$ is calculated with the incident constituents a and b with zero mass. This is a good approximation as long as x_a or x_b are not close to 1. The correct value at zero transverse momentum, from (2.3), is

$$k_a^2 = x_a\left[M_A^2 - \frac{M_{A\bar{a}}^2}{(1-x_a)}\right].$$

(iv) The inclusive cross section $A+B\to C+X$ is given by the incoherent sum over all relevant subprocesses and constituents (a,b)

$$\frac{d^3\sigma}{dp^3} = \sum_{\substack{\text{subprocesses}\\ a+b\to c+\cdots}} \frac{1}{\pi} G_{a/A}(x_a) G_{b/B}(x_b) G_{C/c}(x_C) \frac{1}{x_C^2} \times \frac{\hat{s}}{\pi}\frac{d\sigma(\hat{s})}{dt}\delta(\hat{s}+\hat{t}+\hat{u})\,dx_a\,dx_b\,dx_C\,. \quad (2.13)$$

(v) The structure functions to be used are defined by

$$G_{a/A}(x_a) = \int_0^{\alpha p_T} d\vec{k}_a G_{a/A}(x_a, \vec{k}_a), \quad \text{(see Sec. III)}$$

where $\alpha < 1$, $\alpha p_T \gg O(m)$. In super-renormalizable theories (see Sec. III the integral is insensitive to the upper limit which may be replaced by ∞. This is compatible with the results of approximations (5) and (6) studied earlier since the expansion (2.13) automatically selects kinematics with $\vec{k}_a = \vec{k}_b = 0$.

In order to avoid double counting in (2.13) the undetected particles in the final state of the subprocess $a+b\to c+\{d\cdots\}$ must all share in the high-p_T recoil of the trigger particle (i.e., carry transverse momentum greater than αp_T). This means that the leading subprocesses will produce only two final-state low-mass systems in general, otherwise the cross section is suppressed by extra powers of p_T. Equation (2.13) is represented pictorially in Fig. 6.

We have tested the validity of the hard-scattering expansion (2.13) for the differential cross section and the consequent approximations by considering the $\hat{s}$-channel process in ϕ^3 field theory [Fig. 1(b)]. We compared the exact Feynman graph calculation for the differential cross section with an explicit calculation (subject to the prescription stated above) of the sum of all terms contributed by leading-order subprocesses [shown in Figs. 1(b), 1(e), and 1(f)] to (2.13). The contributions of the subprocesses shown in Figs. 1(e) and 1(f) involve the fragmentation of the particle carrying momentum q into the high-p_T trigger particle k_c. If z is the light-cone variable describing the fragmentation then ($k_T = 0$, $\theta_{cm} = 90°$)

$$q_T = p_T^* - \frac{m^2}{4(1-z)p_T^*}, \quad q^2 = \frac{m^2}{z(1-z)}, \quad (2.14)$$

where

$$p_T^* = [p_T + \sqrt{(p_T^2 + m^2)}]/2z\,.$$

Ignoring mass effects yields $q_T = p_T/z$ but near $z = 1$ this is a bad approximation and in our calculation the exact expressions (2.14) were used. The calculation was done for $s = 640\,000$ GeV^2 and 800 GeV^2, $0.2 \le x_T \le 0.8$. All masses were set equal to 1 GeV. In both cases the agreement between the exact Feynman-graph calculation and the result of summing all leading terms in the hard-scattering expansion was accurate to ~10%.

The results of this section indicate that the simple parton model may be successfully employed to calculate inclusive cross sections as long as we recognize that the high transverse momentum is always produced in a constituent subscatter and not in the wave function of the incident hadrons. The sum over such subscatters then accounts for all the leading contributions from the exact Feyn-

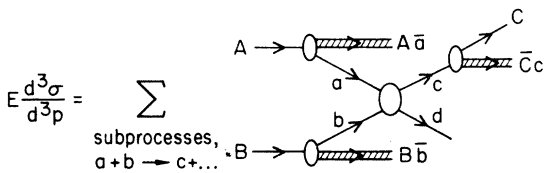

FIG. 6. Representation of hard-scattering expansion.

man-graph calculation while at no stage violating any of the conditions for applicablility of the parton model. In the next section the validity of these results is discussed in the context of renormalizable field theories.

III. VALIDITY OF THE HARD-SCATTERING EXPANSION IN RENORMALIZABLE AND SUPER-RENORMALIZABLE FIELD THEORIES

In the preceding section the hard-scattering expansion was developed by considering explicit examples in ϕ^3 field theory. Because of the superrenormalizability of the interaction, or alternatively because of a dimensionful coupling constant, processes calculated in ϕ^3 field theory exhibit the features of the parton model when they are considered in the appropriate kinematic limit. The situation in renormalizable field theories is more complex and the validity of the hard-scattering expansion and its parton-model nature must be reexamined in the context of these theories and specifically for QED and QCD. We consider the representation for the single-particle inclusive differential cross section given in (2.5). The δ function is accounted for by integrating over x_a and the exact result may be written as

$$E\frac{d^3\sigma}{dp^3}=\int dx_b d\vec{k}_a d\vec{k}_b G(x_a,\vec{k}_a)G(x_b,\vec{k}_b) \times f(x_T,\vec{p}_T,\vec{k}_a,\vec{k}_b,x_b)\,. \tag{3.1}$$

All unnecessary notation has been suppressed and the dependence on quark masses and on coupling constants is implicit. The function $f(x_T,\vec{p}_T,\vec{k}_a,\vec{k}_b, x_b)$ includes all factors resulting from the x_a integration as well as the differential cross section $d\sigma/d\hat{t}$ and the sundry factors which accompany it. Equation (3.1) is still an exact representation of the Feynman integral under consideration and for concreteness we shall consider it in the context either of the ϕ^3 theory $\hat{s}$-pole process of Fig. 1(b) or the QED (QCD) process of Fig. 1(g). We consider the various regions of the $\vec{k}_a$ and $\vec{k}_b$ integrations in (3.1) for fixed $x_T(=2p_T/\sqrt{s}\,)$ in order to define the hard-scattering expansion and to isolate the power dependence of each term in $(1/p_T{}^2)$. For this purpose the functions $G(x,\vec{k})$ are parametrized by [see Eq. (2.4)]

$$G(x,\vec{k})=\frac{G_0(x)}{(\vec{k}^2+m^2)^{1+\epsilon}}\,, \tag{3.2}$$

where ϵ is the dimension of the coupling constant g. The mass scale m is generally x dependent but this makes no difference to the conclusions following. We discuss the situation in which the function $d\sigma/d\hat{t}$ contains four powers of the coupling constant

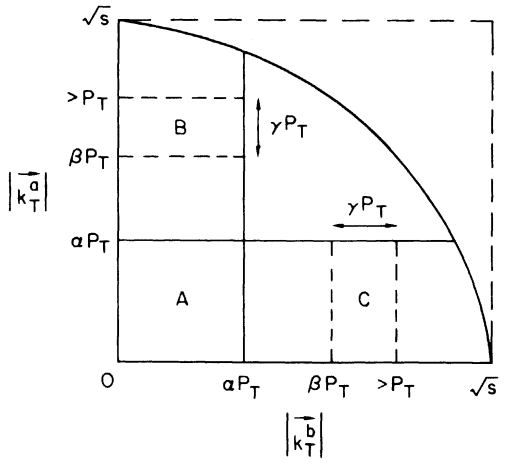

FIG. 7. A, B, C are the main areas of $(\vec{k}_a,\vec{k}_b)$ space contributing to the ϕ^3 field theory inclusive high-p_T scattering. $\alpha,\beta,\gamma\ll 1$, αp_T, βp_T, $\gamma p_T \gg m_q$. These regions correspond to the different subprocesses shown in Fig. 1.

(Born terms) and hence $(1/g^4)f(x_T,p_T,\vec{k}_a,\vec{k}_b,x_b)$ has dimension $(\text{mass})^{-4(1+\epsilon)}$. We isolate terms in the hard-scattering expansion by considering three integration regions $0\le\vec{k}_a\le\alpha p_T$; $\alpha p_T\le\vec{k}_a\le\beta p_T$; $\beta p_T\le k_a\le p_T$, and similarly for $\vec{k}_b$; these regions are shown in Figure 7. [The division of the integration regions can also be made in a covariant manner by using $0\le|k_a{}^2|\le\alpha^2 p_T{}^2$, etc., where $k_a{}^2$ is given in (2.3).] In order to isolate the leading and nonleading contributions we expand the expression (3.1) about $m=0$. However, in order for each term to be well defined at the lower end of the $\vec{k}_a$ and $\vec{k}_b$ integrations a simple inspection of (3.1) shows that we should consider the expansion of

$$m^4E\frac{d^3\sigma}{dp^3}\sim m^{4\epsilon}\int\frac{G_0(x_a)}{(\vec{k}_a{}^2+m^2)^{1+\epsilon}}\frac{G_0(x_b)}{(\vec{k}_b{}^2+m^2)^{1+\epsilon}} \times f(x_T,\vec{p}_T,\vec{k}_a,\vec{k}_b,x_b)dx_b d^2\vec{k}_a d^2\vec{k}_b\,. \tag{3.3}$$

First consider $\epsilon>0$. For $0\le|\vec{k}_a|,|\vec{k}_b|\le\alpha p_T$, the integral is dominated by $1/m^{4\epsilon}$ from the lower end of the $\vec{k}_a,\vec{k}_b$ integration and then, since the only parameter with dimensions is p_T, we find that the expression (3.3) behaves like $1/(p_T{}^2)^{2(1+\epsilon)}$. In the limit $m\to 0$ in (3.1) this is the only term that survives for this region and represents a leading term in the hard-scattering expansion. In ϕ^3 field theory for which $\epsilon=1$, this $p_T{}^{-8}f(x_T)$ term was exhaustively analyzed in the previous section, and for the $\hat{s}$-pole process corresponds to the subprocess of Fig. 1(b). In QED (or QCD) in the tree approximation (no vacuum polarization), $\epsilon=0$, and the integral is only logarithmically divergent in

m. For $0 \leq |\vec{k}_a|, |\vec{k}_b| \leq \alpha p_T$ we then easily find that the leading contribution behaves like $(\ln p_T^2/m^2)^2/p_T^4$. This corresponds to the subprocess explictly illustrated in Fig. 1(g). (An axial or Coulomb gauge is assumed here.)

For $\alpha p_T \leq |\vec{k}_a| \leq \beta p_T$ and no restriction on $\vec{k}_b$ from (3.3) for $\epsilon > 0$ we find that the integrand behaves like $(p_T^2)^{-\epsilon}(m^2)^{-\epsilon}(p_T^2)^{1+\epsilon}$. In the limit of $m \to 0$ this contribution to (3.3) vanishes like $m^{2\epsilon}$ and hence the leading contribution in this region is suppressed by $(m^2/p_T^2)^\epsilon$ relative to the leading terms. Referring to Figs. 1(b) and 1(g), this corresponds to the $2 \to 3$ subprocess $p_A + k_b \to l_a + k_c(\equiv p) + k_d$, where k_a and q share in carrying the large-p_T momentum. In ϕ^3 field theory this is a nonleading contribution since $\epsilon = 1$ and is suppressed by (m^2/p_T^2) factors. In the tree approximation this contribution is however suppressed in QED (QCD) only by $\ln(p_T^2/m^2)$. The region $\beta p_T \leq |\vec{k}_a| \leq p_T/x_T$, $0 \leq |\vec{k}_b| \leq \alpha p_T$ is similarly analyzed, but it is best first to rearrange the representation (3.3) to highlight a new subprocess, namely, that in which k_a is the internal exchange particle. For the $\hat{s}$-pole process in ϕ^3 theory this is illustrated in Fig. 1(e). The $\vec{k}_a$ integration may then be converted to an integration over the low-momentum region of a transverse-momentum variable of a new structure (or fragmentation) function. In the case of Fig. 1(e) this variable is the transverse momentum $\vec{k}_d'$ characteristic of the fragmentation $q \to k_c + k_d$. In Fig. 7 the main regions of contribution A, B, C are illustrated. A corresponds to the subprocess of Figure 1(b) or 1(c). B corresponds to Figs. 1(d) or 1(e), and C corresponds to Fig. 1(f) (this is a leading contribution only in the case of the $\hat{s}$-pole process). The same analysis of course applies to any graphs with the same topology as Figs. 1(c)–1(f) [e.g., Fig. 1(g)].

For $\epsilon > 0$ the upper limit on $\vec{k}_d'$ is not important, but for $\epsilon = 0$, $\ln(p_T^2/m^2)$ factors modified by functions of x_T occur. For both cases in the examples cited we retrieve leading contributions to the Feynman integrals. If we include the effects of vacuum polarization in the QCD calculation then the effective structure function behaves like $1/[\vec{k}^2 \ln(\vec{k}^2/\Lambda^2)]$ in transverse momentum and for the region $0 \leq |\vec{k}_a| \leq \alpha p_T$ the enhancement is only a factor $\ln[\ln(p_T^2/\Lambda^2)/\ln(m^2/\Lambda^2)]$ and not $\ln(p_T^2/m^2)$ as it was in the tree approximation. For QED, the exact incorporation of the vacuum polarization is not understood because of the problems inherent in the Landau singularity.

It is clear that the hard-scattering expansion is most useful in soft field theories with (fixed point) $\epsilon > 0$, such as ϕ^3 theory. In the case of subprocesses which involve hadronic constituents, as in the constituent-interchange model,[3] the effective theory has $\epsilon = 1$ or 2 (for mesons and baryons, respectively) if the underlying quark-field theory is renormalizable. In such models, the transverse-momentum fluctuations are correctly represented by the hard-scattering expansion. In the case of renormalizable theories the enhancement of leading terms is only logarithmic. In QED, the $\ln(s/m_e^2)$ enhancement is responsible for the equivalent-photon approximation.[20] In QCD, the ln ln factors often exponentiate to a power of logarithms in infinite order. The nonleading terms are then only suppressed by a power of logarithms.

Examples of relevant physical processes are examined in the next section in the context of the hard-scattering expansion.

IV. PROTON-PROTON REACTIONS WITH TRANSVERSE FLUCTUATIONS

A. The origin of k_T fluctuations

A very general description of the quark distribution functions $G(x, \vec{k}_T)$ can be based on the decomposition of the hadronic wave function shown in Fig. 8, corresponding to the different constituents which balance the quarks transverse momentum. This series generates an effective $\vec{k}_T$ distribution at large $\vec{k}_T$

$$\frac{dn}{dk_T^2} \sim \frac{\alpha_c(k_T)}{k_T^2} + \frac{c_4 m^2}{k_T^4} + \frac{c_6 m^4}{k_T^6} + \cdots , \tag{4.1}$$

where the power of k_T^{-2} increases with the number of constituents sharing the recoil. The first term from QCD gluon recoil holds for $k_T^2 < O(p_T^2)$. The k_T^{-4} from quark or antiquark recoil is a standard CIM contribution. The general form for the G

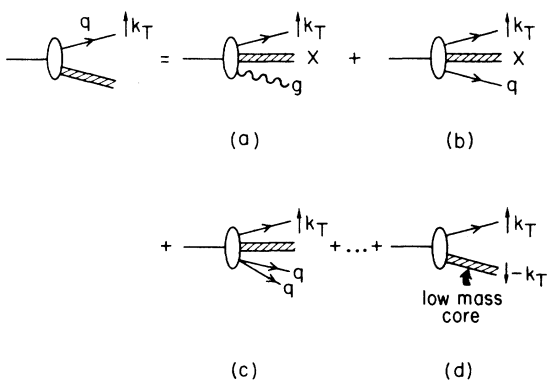

FIG. 8. The origin of quark transverse momentum in the hadron wave function showing the various recoil constituents and the remaining low-mass, low-k_T core X. See Eq. (4.1).

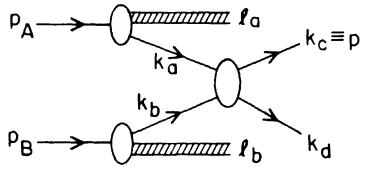

FIG. 9. Generic hadron+hadron → (high-p_T trigger) $+X$.

function in the case of Fig. 8(d), where the recoil system contains n constituents, is[18]

$$\frac{d^2N}{dx\,dk_T^{\,2}} = g(x,k_T) \propto \frac{(1-x)^{2n-1}}{[k_T^{\,2}+M_{\rm eff}(x)]^{2n}} . \tag{4.2}$$

These rules follow from the power-law behavior of the minimally connected Bethe-Salpeter wave function from the QCD tree graphs. Here

$$M_{\rm eff}^{\,2}(x) = xM_{\rm core}^{\,2} + (1-x)M_q^{\,2} - x(1-x)M_p^{\,2} .$$

This describes the emission of a quark of mass M_q recoiling against a system of mass $M_{\rm core}$. The core mass is a parameter of the model and in order to fit the Regge behavior of the cross section, the core mass must behave[21] as $M_{\rm core}^{\,2} \sim (M_c^0)^2/x$. The form of Eq. (4.2) ensures the covariance of the final results. In the case where there are spectators X at low k_T, e.g., Fig. 8(a)–8(c), the distribution functions can be obtained from a two-step process where $p \to H+X$, and the system H produces the quark at large k_T with no low-k_T spectators. This is consistent with the hard-scattering expansion since the system H is at low k_T.

We can now consider the effect on various physical pp large-p_T processes which follow from fluctuations of the general form (4.2). In each case we have calculated the differential cross section in the framework of the hard-scattering model shown diagramatically in Fig. 9 for which the notation of Fig. 1(a) is retained. Where appropriate the distributions $G(x)$ for q and $\bar{q}$ were taken from fits to the SLAC deep-inelastic lepton-hadron scattering data.[14]

B. Drell-Yan process

The simplest process to consider for illustration of the effects of k_T fluctuations is the Drell-Yan process $pp \to \mu^+\mu^- X$ in which the subprocess is $q\bar{q} \to \mu^+\mu^-$. Let us first consider the case in which the distribution is given by Eq. (4.2) with $n \geq 2$. This corresponds to the situation in which all the spectator quarks recoil as a low-mass system as shown in Fig. 8(d). In Fig. 10 the single-μ invariant cross section derived from this process as defined by (2.5) with exact kinematics is plotted against p_T for $s = 600$ GeV^2, $\theta_{\rm c.m.} = 90°$. The

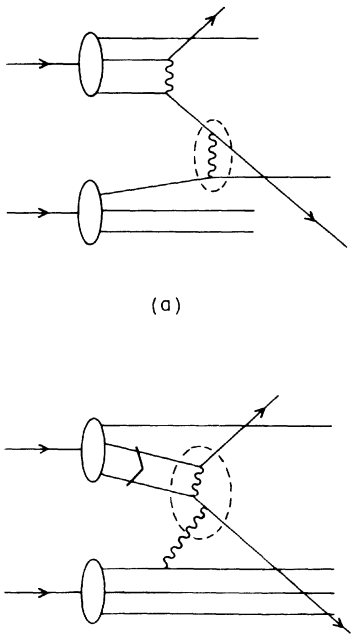

FIG. 10. Examples of subprocesses contributing to the hard-scattering expansion contained in the $qq \to qq$ subscattering process for proton-proton scattering. (a) quark+quark → quark+quark (quark recoil contribution). (b) diquark+gluon → quark+quark.

approximate calculation ignoring the transverse-momentum fluctuations (i.e., the standard parton model) is not shown since it is negligibly different from the exact calculation. This is expected since there are no other leading subprocesses in this particular model of single-muon production when $n \geq 2$ in (4.2). This feature will hold true in any model where the k_T fall off is sufficiently fast. At $p_T = 5$ GeV/c, this single-muon production (including color) is a factor of about 3 below the data[23] which is also shown in Fig. 10. The anomalously large average transverse-momentum distribution of dileptons,[24] which grows with the pair mass, has prompted some authors to suggest that the parton transverse-momentum fluctuations are quite large.[10-12] These fluctuations might then be expected to give a boost to the single-lepton cross section. Such an effect can only occur if there are new hard-scattering subprocesses (e.g., involving quark or gluon recoil) which can compete with the $q\bar{q} \to \mu^+\mu^-$ (lepton recoil) subprocess at moderate values of $p_{T(\mu)}$. Such processes can be $q\bar{q} \to g\gamma^*$,[25] [which is implicit in Fig. 8(a)], $qg \to \gamma^* q, qq \to qq\gamma^*$, $Mq \to \gamma^* q$. The last subprocess [shown in Fig. 11(b)] is that considered by Duong-van, Vasavada,

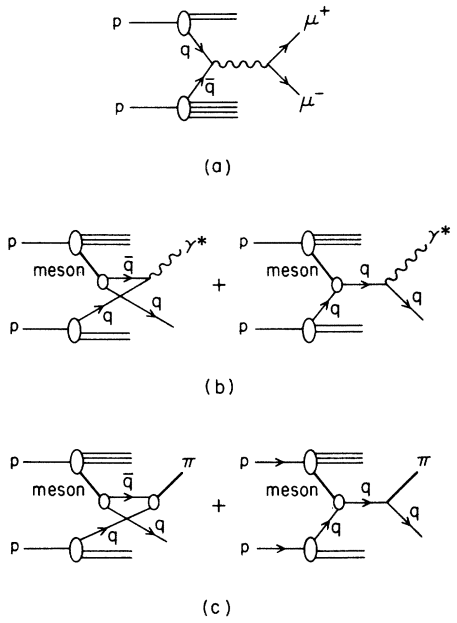

FIG. 11. (a) Drell-Yan subscatter $q\bar{q} \to \mu^+\mu^-$. (b) CIM subscatter $Mq \to \gamma^*(\to \mu^+\mu^-)q$. (c) CIM subscatter $Mq \to \pi q$.

and Blankenbecler[15] and by Fontannaz.[29] This model fits the lepton-pair transverse-momentum distribution as a function of pair mass, and the normalization[15] of the subprocess $Mq \to \gamma^* q$ is compatible with the normalization[3] of $pp \to \pi X$ at large p_T from the CIM subprocess $Mq \to Mq$.

In principle, the effect of these subprocesses is included in the exact Feynman-diagram calculation of the $pp \to \mu X$ cross section using the first two terms of Eq. (4.1).

The subprocess $Mq \to \gamma^* q$ subsumes the Drell-Yan subprocess [which corresponds to the first (crossed) graph of Fig. 11(b)] when the final-state quark has small transverse momentum and hence may be counted as part of the low-mass core. From the discussion of IIC the crossed graph includes the effect of transverse fluctuations of the antiquark constituent in the Drell-Yan process which arise by recoil against a single quark in the proton wave function. The second (uncrossed) graph of Fig. 11(b) which is negligible in the Drell-Yan limit (i.e., zero transverse momentum of the muon pair) is necessary for preserving QCD gauge invariance. Hence this reaction contains extra contributions which represent the effect of transverse fluctuations in the Drell-Yan process as well as containing the Drell-Yan process itself. As we cautioned in IIC we should not double count by including the $q\bar{q} \to \gamma^*$ subprocess indpendently. We remark that the uncrossed graph of Fig. 11(b) is a new hard-scattering contribution which does not contain $q\bar{q}$ annihilation and whose contribution would be ignored in a naive approach to the effect of transverse fluctuations which assigns a transverse-momentum distribution to the antiquark in the structure function. The single-lepton transverse-momentum distribution for this model is plotted in Fig. 10 and the results reflect the extra p_T^{-6} contribution included in the $Mq \to \gamma^* q$ subprocess. At large p_T this extra effect vanishes and the results for single-μ production from $q\bar{q} \to \gamma^*$.

The contributions from the (p_T^{-4}) QCD subprocess $qg \to \gamma^* q$, $q\bar{q} \to g\gamma^*$, etc., will also increase the single-μ yield. Using the hard-scattering expansion, those will yield further p_T^{-4} contributions at fixed x_T and $\theta_{\text{c.m.}}$ and will renormalize the $q\bar{q} \to \mu^+\mu^-$ contribution to single muons. However, because of the trigger bias effect[26] (from $\gamma^* \to \mu^+\mu^-$ fragmentation) these contributions are relatively suppressed. These events are interesting and can be distinguished because they contain a recoil quark or gluon jet[25] rather than a recoil muon (as is the case for $q\bar{q} \to \mu^+\mu^-$).

C. Single-pion production

We have analyzed the leading constituent-interchange process for the production of prompt pions $pp \to \pi X$ in a way similar to the analysis of the previous subsection. The subprocess under consideration, meson$+q \to \pi q$, is shown in Fig. 11(c) and the quark is given a mass of 1 GeV. The full distribution function (i.e., including transverse momentum) of the meson in the proton is taken from Ref. 3.

The inclusion of transverse fluctuations with rapidly falling distributions [$N \geq 3$ in (4.2)] makes a negligible contribution to the differential cross section as we should expect in the light of the previous discussion. To discuss the effect of constituent transverse fluctuations in general, we need to discuss subprocesses such as meson+meson$\to \pi q\bar{q}$. A simple power analysis shows that the contribution falls like p_T^{-12} compared to the leading p_T^{-8} CIM contribution. Thus the effect is more rapidly damped than the corresponding modification by nonleading subprocesses (e.g., $Mq \to \gamma^* q$) in direct μ production.[27]

D. Quark-quark scattering subprocesses

We can also investigate the effects of transverse fluctuations with respect to the QCD scattering processes, $qq \to qq$, $qg \to qg$, $gg \to gg$, which are expected to be particularly relevant to high-p_T jet production in hadron collisions.

As we emphasized in the introduction, the use of on-shell constituent kinematics cannot be justi-

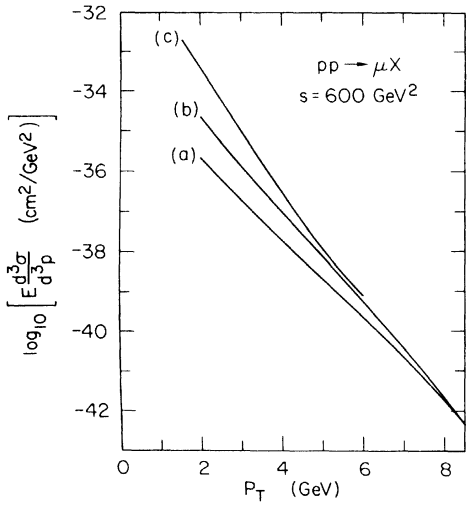

FIG. 12. $Ed^3\sigma/dp^3$ for single-μ production at high p_T for $s = 600$ GeV^2 (a) Drell-Yan, $q\bar{q} \to \mu^+\mu^-$. (b) CIM, $Mq \to (\mu^+\mu^-)q$. (c) Data (Ref. 23).

fied and requires arbitrary cutoffs in the calculations. In order to see explicitly the source of difficulties in this procedure we have calculated the QCD $qq \to qq$ subprocess contributions using the on-shell parameterization (2.8).

If transverse fluctuations are now introduced, the regions of integrations surrounding the $\hat{t}$ and $\hat{u}$ poles contribute. This singular enhancement must be regulated; e.g., by a fictitious gluon mass or a linear cutoff in the integration region. The consequent result is thus not only regulator dependent but is dominated by a region of integration, which in fact does not actually contribute in the exact calculations.

The features of such calculations are exemplified in Figs. 12 and 13, the effects of various on-shell $qq \to qq$ models are compared with the calculations with exact off-shell kinematics. Four cases are considered: (1) no transverse momentum; (2) a rapidly falling distribution $\sim k_T^{-8}$ derived from Eq. (4.2) with $2n = 4$; (3) a normalized $\exp(-3k_T)$ distribution where $\langle k_T \rangle = \frac{2}{3}$ GeV; (4) a normalized $\exp(-3k_T^2)$ distribution with $\langle k_T \rangle = 0.51$ GeV. The gluon mass was set to M_q or $\sqrt{10}M_q$, with $M_q = 300$ MeV.

In Fig. 12 we plot the contributions to the inclusive cross section $Ed^3\sigma/d^3p dx_a$ at $s = 800$ GeV^{-1}, $p_T = 4$ GeV/c, $\theta_{c.m.} = 90°$ as a function of x_a where all other variables have been integrated over. The results for cases (1), (2) with either off-shell or on-shell kinematics all coincide at the scale used in the figure and are shown as curve (a). Curve (b) represents case (3) with off-shell kinematics and curves (c) and (d) represent case (3) with on-shell kinematics for $M_g = M_q, \sqrt{10}M_q$, respectively. The exact kinematics calculation shown as curve (a) shows that the region of $x_a \leq 0.08$ (which is the kinematic boundary) does not contribute to the cross section for any choice of transverse fluctuations. However, for case (3) which has a moderately falling $\exp(-3k_T)$ distribution, the on-shell calculation receives large contributions from the $x_a \sim 0$ region which is sensitive to the $\hat{t}^{-2}$ pole. The effect of this region is governed strongly by the gluon mass as illustrated in cruves (c) and (d) of Fig. 13 which correspond to the two cited choices of M_g. Near $x_a = 0$ the ratio of the two curves is 1:100, reflecting the M_g^{-4} dominance of the cross section. In case (2), for on-shell kinematics, the $x_a \to 0$ region contributes but is numerically suppressed for these values of M_g by the strongly damped distribution.

The corresponding inclusive cross sections for $pp \to q + X$ are shown in Fig. 13. The on-shell calculation with e^{-3k_T} is anomalously high [curve (d)] compared to the off-shell kinematics calculation with e^{-3k_T} [curve (b)]. Curve (a) represents cases (1) and (2) and cruve (c) represents case (4) with either off-shell or on-shell kinematics. It is clear that the spurious on-shell contribution is not physical but is a result of the breakdown of the on-shell approximation when including transverse fluctuations. The method of regulating the pole is arbitrary and tantamount to choosing the final result at will.

As we have discussed in Secs. II and III, the true

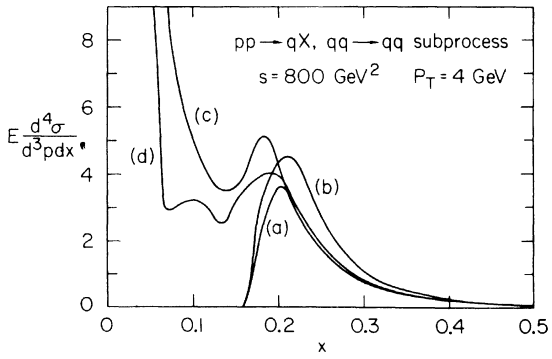

FIG. 13. $E(d^4\sigma/dp^3dx)$ versus x for quark-jet production ($qq \to qq$) for $s = 800$ GeV^2 and $p_T = 4$ GeV where x is the light-cone variable of one constituent. The normalization is arbitrary. The curves shown are (a) Cases (1) and (2) (given in Sec. IV D) for either on-shell or off-shell kinematics (these all coincide at this scale). (b) Off-shell kinematics with normalized e^{-3k_T} distribution (case 3). (c) On-shell kinematics with normalized e^{-3k_T} distribution (case 3) for $M_g = M_q$. (d) As (c) but for $M_g = \sqrt{10}\, M_q$.

effect of transverse-momentum fluctuations can be determined by the hard-scattering expansion. From this point of view, it is clear why the inclusion of transverse-momentum fluctuations with exponential or power-law k_T^{-n} ($n>4$) distributions causes negligible change in the differential cross sections. These contributions can be identified with nonleading processes in the hard-scattering expansion relative to the leading p_T^{-4} terms. As discussed in the introduction to this section with reference to Fig. 8 and Eq. (4.1) it is possible to generate less steeply falling distributions by recoiling the active constituent against other constituents in the incoming hadrons. The leading terms correspond to simply gluon recoil which can be analyzed from the Feynman graphs by considering all $2\to3$ subprocesses in QCD, e.g., $qq\to qqg$. To leading logarithmic order, the $2\to3$ contributions can be represented by all possible $2\to2$ QCD hard-scattering subprocesses. As shown in Fig. 2(a) and 2(b) the effects of gluon bremsstrahlung in qq scattering can be reinterpreted in terms of the hard-scattering subprocess $qq\to qq$ with gluon emission along the initial and final quark lines, plus the subprocess $qg\to qg$. Figure 2(a) can be identified with the jet topology of standard $qq\to qq$ scattering. Figure 2(b) is distinguished by the appearance of the gluon jet in place of a quark jet. The remainder of the $2\to3$ $qq\to qqg$ subprocess corresponds to three-jet production processes and is a logarithmically nonleading term in the hard-scattering expansion. These contributions include the effects associated with the first term of Eq. (4.1) and thereby treat the transverse-momentum distribution of quarks in a consistent gauge-invariant way.

All of the above QCD Born contributions generate only p_T^{-4} contributions to the inclusive cross-sections modulo logarithms. Contributions with higher p_T^{-2} are generated by diagrams such as those shown in Fig. 14 where a quark recoils in the wavefunctions via the exchange of internal gluons. One of these contributions [Fig. 10(b)] can be identified with diquark+glue$\to qq$ subprocesses which are suppressed modulo logarithms by a factor of f^2/p_T^2 in QCD where f is a dimensional constant which arises from the integration over the relative momentum of the diquark system.

In a similar manner one can generate higher-power fall-off contributions corresponding to the other terms in Eq. (4.1), Fig. 8. These correspond to subprocesses based on hadron-quark interactions, such as $Mq\to Mq$ [see Fig. 2(c)]. Although such contributions have nominal p_T^{-8} fall off, they can temporarily dominate the QCD p_T^{-4} terms at moderate p_T in single-particle production because of (a) the trigger-bias effect[26] [p_T^q or $p_T^g > p_T$ (trigger)] and (b) possible enhancements due to the binding of color singlets.

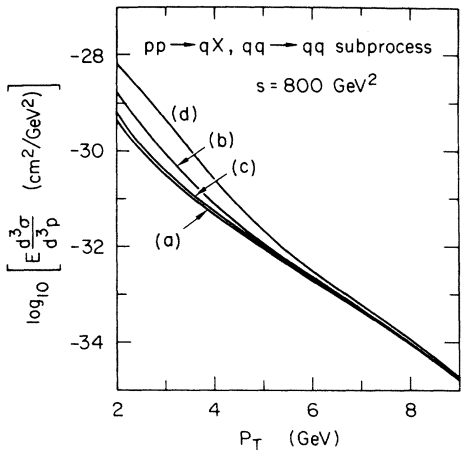

FIG. 14. $E(d^3\sigma/dp^3)$ for production of a quark jet at 90° versus p_T for $s=800$ GeV^2. The curves shown are (a) As (a) in Fig. 13. (b) As (b) in Fig. 13. (c) Normalized $e^{-3k_T^2}$ distribution [case (4) Sec. IV D] for either on-shell or off-shell kinematics. (d) As (d) in Fig. 13.

V. CONCLUSIONS

As we have shown in this paper, the effects of constituent transverse-momentum fluctuations are in general very complex. The exact treatment requires consideration of off-shell and coherence effects and ultimately subprocesses involving multijet final states. The hard-scattering expansion, however, can be used to theoretically isolate the origin of all large transverse-momentum exchanges within a set of hard-scattering subprocesses, yielding a tractable, systematic expansion of the inclusive cross section at high p_T. In the case of ϕ^3 field theory or the constituent-interchange model (which focuses on quark-hadron scattering subprocesses), the hard-scattering expansion yields a series in inverse powers of p_T^2 at fixed x_T. Within the expected numerical accuracy, the sum of the leading parton-model terms in the hard-scattering expansion for ϕ^3 theory was shown to reproduce the cross section obtained from an exact calculation of the Feynman amplitudes. The indication from perturbation theory is that in the case of asymptotically free theories such as QCD, the enhancement of leading terms is only logarithmic.

We have also shown that the effect of transverse-momentum fluctuations in qq-scattering calculations are of minor importance in inclusive cross sections if (1) the correct off-shell kinematics are used, and (2) the k_T distribution functions reflect nonleading subprocesses.[28] We emphasize

that the neglect of the essential off-shell nature of the constituents when considering the transverse-momentum distribution violates momentum conservation and allows otherwise forbidden kinematic regions such as $\hat{t}=0$ or small x_a and x_b to contribute. These pathologies in turn lead to divergencies which must be arbitrarily regulated.

Of course for fast-falling distributions such as $\exp(-3k_T^2)$, it can be seen from Fig. 13 that for on-shell kinematics the contributions from small x_a and x_b are negligible although nonzero. The consequence of this fact is, however, that only small values of k_T are relevant and as shown in Fig. 14, curve (c), the correction at moderate p_T (~3–4 GeV) is less than the order of 30%. This result can be easily verified by using the mean-value theorem for integrals which dictates the replacement $(p_T^2+m^2)\to(p_T-\bar{k}_T)^2+m^2$ in the final answer where $\bar{k}_T\sim\langle k_T\rangle$.

Alternatively, for slowly falling distributions with on-shell kinematics spurious contributions are picked up from singular regions as seen from Figs. 13 and 14. This is clearly incorrect. A comparison with the canonical form for the differential cross section

$$E\frac{d^3\sigma}{dp^3}\propto p_T^{-4}(1-x_T)^7$$

at $\Theta_{\mathrm{c.m.}}=90^\circ$ for $qq\to qq$ is shown in Fig. 15. For the $\exp(-3k_T^2)$ distribution, even though $\langle k_T\rangle$ ~ 0.51 GeV, the deviation from the curve with no smearing [curve (a)] is of the same order of magnitude as the deviations induced by mass effects and rapidly disappear with increasing p_T. For the $\exp(-3k_T)$ distribution, which falls off much more slowly, the off-shell curve (b) in Fig. 15 does exhibit an increase from the canonical form at low

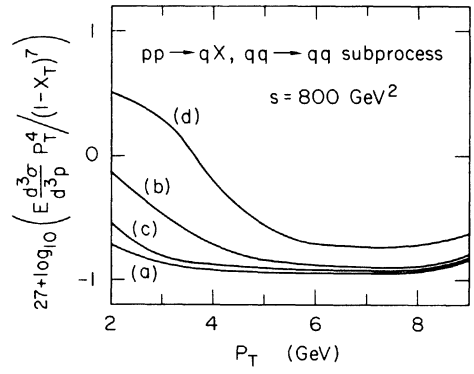

FIG. 15.

$$27+\log_{10}\left[E\frac{d^3\sigma}{dp^3}p_T^4/(1-x_T)^7\right]$$

for the cases (a)–(d) given in Fig. 14.

p_T. As we have already argued the contributions associated with increases of this kind should be identified with other, nonleading, subprocesses in the systematic way described in Sec. III.

It should be emphasized that it is in principle impossible to treat constituent transverse-momentum fluctuations as a phenomenon distinct from the hard-scattering subprocess; the same basic interactions must account for both. For example, as has been discussed in Refs. 15 and 29 and in Sec. IV, the p_T distribution of high-mass lepton pairs in $pp\to l^+l^-X$ which is often ascribed to the intrinsic quark and antiquark distributions in the proton is, from a different perspective, the distribution for high-p_T massive-photon reactions which is usually considered as arising from a standard hard-scattering subprocess. Thus theoretically it is most advantageous to localize all the large-transverse-momentum exchanges explicitly within hard-scattering subprocesses.

From another perspective, the central difficulty of large-k_T fluctuations is the fact that they cannot be treated as a classical effect. This can be seen in the framework of the Drell-Yan time-ordered perturbation-theory analysis.[30] The lifetime of a constituent is of the order $\tau_{\mathrm{life}}=x(1-x)P/k_T^2$ and the time of interaction is of order $\tau_{\mathrm{int}}=P/(p_T-k_T)^2$. Thus for large k_T, τ_{life} can be less than τ_{int}; just the reverse of what is assumed for the validity of the parton-model expansion. In covariant language a far off-shell line cannot be considered as a classical particle, but must be considered as part of a larger process.

Finally, our considerations in this paper suggest a computational procedure which in principle yields the correct asymptotic form for cross sections at large p_T and takes into account the complications of the hadronic wave functions:

(1) Starting from a given field theory, one constructs the coupled set of multiparticle wave functions[31] $\Psi_n(k_{Ti},x_i)$ in time-ordered perturbation theory using the standard light-cone variables.[16] The effective potential is covariantly cut off so that intermediate states which are far off shell are excluded[32]

$$[M^2-H_0]\Psi=\Theta(M^2-H_0+\alpha^2p_T^2)V\Psi\,, \qquad (5.1)$$

where $H_0=\sum_i(m_i^2+k_{Ti}^2)/x_i$. As in Sec. III, we define the quantity $\alpha^2\ll 1$ in order to separate explicit hard-scattering processes from the implicit soft processes already contained in the wave function via (5.1). Given these wave functions, one can unambiguously compute the structure functions specific to the constituents of each interacting hadron.

(2) All relevant hard-scattering contributions to the large-p_T process are now computed using Eq. (2.13). A given hard-scattering subprocess is in-

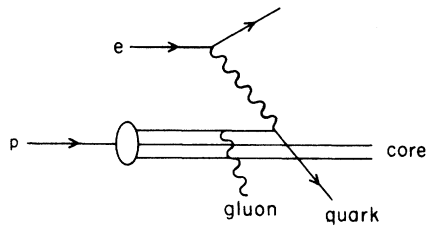

(a)

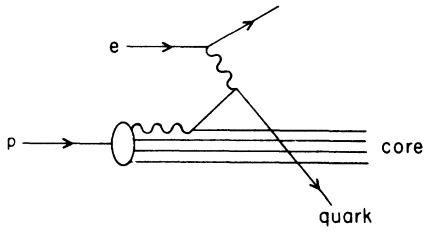

(b)

FIG. 16. Contributions to ep scattering from (a) $|qqqg\rangle$ wave functions and (b) $|qqqq\bar{q}\rangle$ wave functions.

cluded in the perturbation expansion only if

$$\left|M^2 - \sum_i (k_{Ti}^2 + m_i^2)/x_i\right| \geq \alpha^2 p_T^2 , \qquad (5.2)$$

where the sum is over the constituents of the bound state of mass M; i.e., all large energy denominators are isolated in subprocess. For an exact calculation the subprocess cross section itself must be computed with the correct off-shell parametrization. This, however, is only a correction of order α.

An example of this procedure applied to deep-inelastic ep scattering is illustrated in Fig. 16. If the energy denominator for the indicated intermediate state in Fig. 16(a) or 16(b) satisfies the criteria (5.2) with $\alpha^2 p_T^2 \sim \alpha^2 Q^2$, then these diagrams represent the hard-scattering contributions (a) $eq \to eqg$ and (b) $eg \to eq\bar{q}$. Otherwise these contributions are automatically included in the $eq \to eq$ subprocess with the respective $|qqqg\rangle$ and $|qqqq\bar{q}\rangle$ wave functions satisfying Eq. (5.1). Of course, when one builds phenomenological models, the sum of contributions from all subprocesses together with the assumed form of the wave functions and resulting distributions $G_{a/A}(x, \vec{k}_T, Q^2)$ must match the observed deep-inelastic lepton-scattering cross sections.

The above procedure, specialized to electron scattering on a quark target, reproduces the Altarelli-Parisi[33] equations for leading logarithms in QCD. More generally this procedure allows one to sort out the contributions which can be associated with the bound-state wave functions (including scaling violations) from those which can be associated with large momentum transfer, and in principle accounts for all nonleading terms.

ACKNOWLEDGMENTS

We than R. Blankenbecler, J. Gunion, and G.P. Lepage for interesting and useful conversations. R. R. H. would like to thank the Lindemann Trust for their support. The numerical calculations in this paper were performed using VEGAS a Monte Carlo multidimensional integration program developed by G. P. Lepage.[35] This work was supported in part by the U. S. Department of Energy.

*Present address: Physics Department, Brown University, Providence, R. I., 02912.

[1]S. Berman, J. Bjorken, and J. Kogut, Phys. Rev. D 4, 3388 (1971). For a review of this subject, with many references, see D. Sivers, S. J. Brodsky, and R. Blankenbecler, Phys. Rep. 23C, 1 (1976); and S. Ellis and R. Stroynowski, Rev. Mod. Phys. 49, 753 (1977).

[2]The present experimental status is reviewed by H. Bøggild, in *Proceedings of the VII International Symposium on Multiparticle Dynamics, Kaysersberg, 1977*), (Centre de Recherches, Nucleaires, Strasbourg, France, 1977, p. B-1; M. Della Negra, CERN Report also ISR discussion meetings Nos. 17, 19, 21.

[3]R. Blankenbecler, S. J. Brodsky, and J. F. Gunion, Phys. Lett. B39, 649 (1972); B42, 461 (1973); Phys. Rev. D 12, 3469 (1975); 2652 (1972); 18, 900 (1978).

[4]R. D. Field and R. P. Feynman, Phys. Rev. D 15, 2590 (1977); Nucl. Phys. B136, 1 (1978); R. P. Feynman, R. D. Field, and G. C. Fox, *ibid.* B128, 1 (1977); R. D. Field, invited talk presented to the American Physical Society, San Francisco, 1978 (unpublished).

[5]P. V. Landshoff and J. C. Polkinghorne, Phys. Rev. D 8, 4157 (1973); 10, 891 (1974).

[6]M. Della Negra *et al.*, Nucl. Phys. B127, 1 (1977). For other calculations using on-shell constituent scattering see also M. Glück, J. F. Owens, and E. Reya, Florida State Report, 1977 (unpublished); J. Ranft and G. Ranft, CERN Report No. TH2369, 1977 (unpublished) and Ref. 4.

[7]M. G. Albrow *et al.* (British-French-Scandinavian Collaboration) (unpublished). See also H. Bøgglid, Ref. 2.

[8]C. Bromberg *et al.*, Phys. Rev. Lett. 38, 1447 (1977) and (unpublished).

[9]J. G. Branson *et al.*, Phys. Rev. Lett. 38, 1334 (1977);

D. C. Hom *et al.*, *ibid.* 37, 1374 (1976); L. Kluberg *et al.*, *ibid.* 37, 1451 (1976); K. J. Anderson *et al.*, *ibid.* 37, 799 (1976).

[10]E. M. Levin and M. G. Ryskin, Zh. Eksp. Teor. Fiz. 69, 1537 (1975) [Sov. Phys. JETP 42, 783 (1975)].

[11]B. L. Combridge, Phys. Rev. D 12, 2893 (1975).

[12]Many authors have discussed the effects of transverse fluctuations on Drell-Yan production of lepton pairs. G. Altarelli, G. Parisi, and R. Petronzio, CERN Report No. TH-2413-CERN, 1977 (unpublished); M. Duong-Van, Report No. SLAC-Pub-1819, 1976 (unpublished); M. Fontannaz and D. Schiff, Orsay Report No. LPTHE 77/23, 1977 (unpublished); J. F. Gunion, Phys. Rev. D 14, 1400 (1976); 15, 3317 (1977); I. Hinchliffe and C. H. Llewellyn Smith, Phys. Lett. 66B, 281 (1977); K. Kinoshita *et al.*, *ibid.* 68B, 355 (1977); J. B. Kogut, *ibid.* 65B, 377 (1977); C. S. Lam and T. M. Yan, *ibid.* 71B, 173 (1977); P. V. Landshoff, *ibid.* 66B, 452 (1977); P. V. Landshoff and D. M. Scott, Nucl. Phys. B131, 172 (1977); D. E. Soper, Phys. Rev. Lett. 38, 461 (1977).

[13]J. D. Bjorken, Phys. Rev. D 8, 3098 (1973); S. D. Ellis and M. B. Kislinger, *ibid.* 9, 2027 (1974); G. Preparata and G. Rossi, Nucl. Phys. B111, 111 (1976). G. Ranft and J. Ranft, Report No. KMU-HEP-77-04, 1977 (unpublished); R. C. Hwa, A. J. Speissbach, and M. J. Teper, Phys. Rev. Lett. 36, 1418 (1976); B. L. Combridge, J. Kripfganz, and J. Ranft, Phys. Lett. 70B, 234 (1977).

[14]R. Blankenbecler *et al.*, in *High Energy Particle Interactions*, proceedings of the Triangle Conference, Smolenice, Czechoslovakia, 1975, edited by D. Krupa and J. Pisut (Veda, Bratislava, 1976), Vol. 2, p. 35. See also G. R. Farrar, Nucl. Phys. B17, 429 (1974). G. Chu and J. F. Gunion, Phys. Rev. D 10, 3672 (1974).

[15]M. Duong-Van, K. V. Vasavada, and R. Blankenbecler, Phys. Rev. D 16, 1389 (1977); C. Sachrajda and R. Blankenbecler, *ibid.* 12, 3624 (1975).

[16]Sivers *et al.* (Ref. 1), Appendix A.

[17]E. Byckling and K. Kajantie, *Particle Kinematics* (Wiley, New York, 1973), Chap. 4.

[18]S. J. Brodsky and G. Farrar, Phys. Rev. Lett. 31, 1153 (1973); Phys. Rev. D 11, 1309 (1975). V. Matveev, R. Muradyan, and A. Tavkhelidze, Lett. Nuovo Cimento 7, 719 (1973). Spectator-counting rules are given in R. Blankenbecler and S. J. Brodsky, Phys. Rev. D 10, 2973 (1974); J. Gunion, *ibid.* 10, 242 (1974).

[19]S. D. Drell, D. Levy, and T. M. Yan, Phys. Rev. 187, 2159 (1969); Phys. Rev. D 1, 1035 (1970).

[20]R. H. Dalitz and D. R. Yennie, Phys. Rev. 105, 1598 (1957). See also Ref. 33.

[21]P. V. Landshoff, J. C. Polkinghorne, and R. D. Short, Nucl. Phys. B28, 222 (1971); S. J. Brodsky, F. E. Close, and J. F. Gunion, Phys. Rev. D 8, 3678 (1973). The results in this section are not sensitive to the choice of M_c^0, which we take as order 1 GeV.

[22]Figures 2(a) and 9(a) contain different contributions to the full quark structure function relevant to the $qq \to qq$ subprocess scatter.

[23]J. P. Boymond *et al.*, Report No. EF1-74-24 (unpublished).

[24]L. M. Lederman, lectures delivered at the Cargèse (Corsica) Summer Institute, 1977 (unpublished).

[25]S. J. Brodsky, W. Caswell, and R. R. Horgan, work presented by S. J. Brodsky, in *Color Symmetry and Quark Confinement*, Vol. III of the proceedings of the XII Rencontre de Moriond, edited by J. Trân Thanh Van (Editions Frontières, Paris, 1977).

[26]S. D. Ellis, M. Jacob, P. V. Landshoff, Nucl. Phys. B108, 93 (1976); see also J. D. Bjorken and G. R. Farrar, Phys. Rev. D 9, 1449 (1974).

[27]Another contributing process is $qq \to \pi qq$ with meson exchange. This is a contribution to qq scattering with quark fragmentation and is still of order p_T^{-8}. A simple estimate of the magnitude of this process shows that its contribution is negligible but formally it is included in the hard-scattering expansion for quark-quark scattering.

[28]The effect of k_T fluctuations using off-shell kinematics has also been considered by R. Ratio and R. Sosnowski, Helsinki University Report, 1977 (unpublished), and M. Chase, Cambridge Report, 1977 (unpublished). See also J. Kripfganz and G. Ranft, TH.2398-CERN, 1977 (unpublished).

[29]M. Fontannaz, Phys. Rev. D 14, 3127 (1976).

[30]S. D. Drell and T. M. Yan, Phys. Rev. Lett. 25, 316 (1970) and Ann. Phys. (N. Y.) 66, 578 (1971).

[31]S. Weinberg, Phys. Rev. 150, 1313 (1966); for applications to renormalizable theories see S. J. Brodsky, R. Roskies, and R. Suaya, Phys. Rev. D 8, 4574 (1973).

[32]An analysis which uses a similar truncation is given by K. J. Kim, Mainz Report No. MZ-TH 78/1 (unpublished).

[33]G. Altarelli and G. Parisi, Nucl. Phys. B126, 298 (1977).

[34]An example of QED perturbation theory which separates hard and soft components in the bound-state kernel is given by W. E. Caswell and G. P. Lepage, SLAC-PUB-2080 (unpublished).

[35]G. P. Lepage, J. Comp. Phys. 27, 92 (1978).

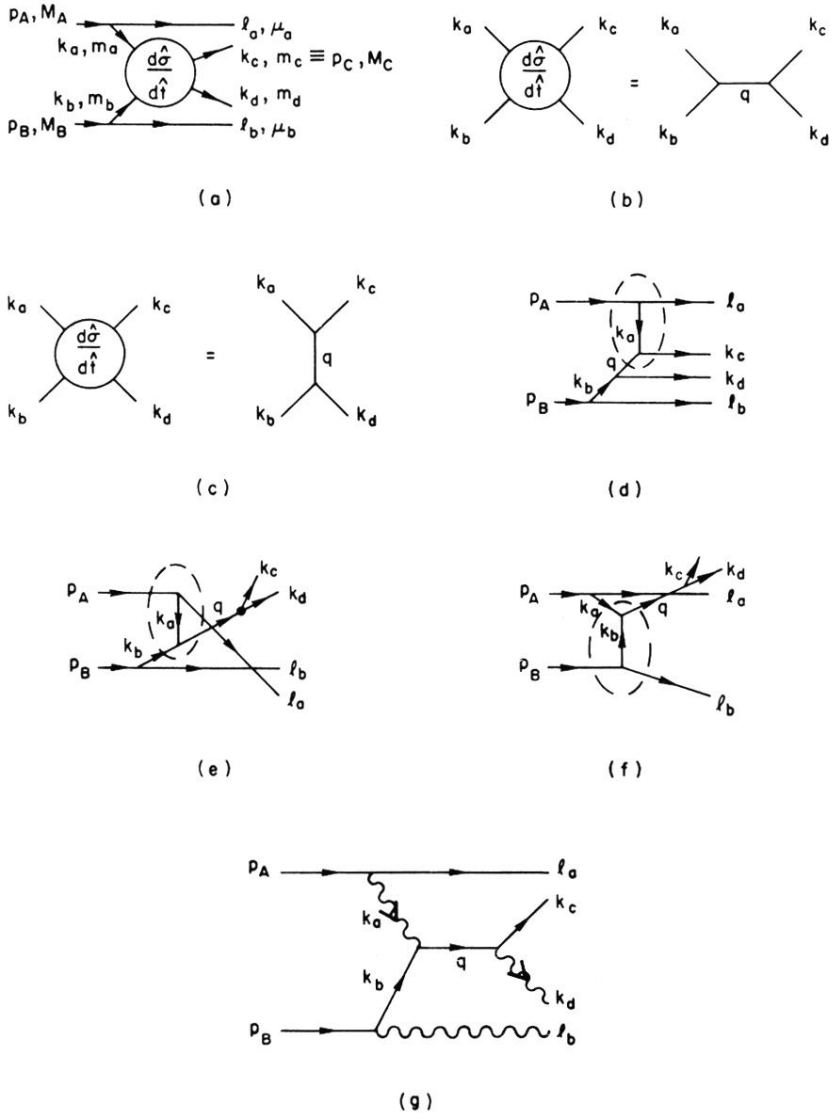

FIG. 1. Contributions to the hard-scattering process: (a) Example of hard-scattering subprocess and definition of momenta. (b) $\hat{s}$-pole subprocess in ϕ^3 field theory. (c) $\hat{t}$-pole subprocess in ϕ^3 field theory. (d) The subprocess other than that of Fig. 1(c) contributing in leading order to the $\hat{t}$-pole hard-scattering expansion in ϕ^3 field theory. (e) and (f): The two subprocesses other than that of Fig. 1(b) contributing in leading order to the $\hat{s}$-pole hard-scattering expansion in ϕ^3 field theory. (g) QCD (or QED) analog of the ϕ^3 field theory $\hat{s}$-pole scattering process.

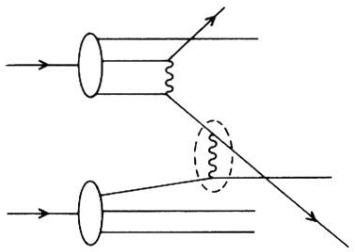

(a)

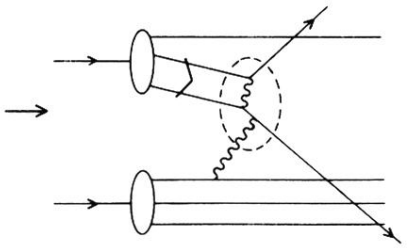

(b)

FIG. 10. Examples of subprocesses contributing to the hard-scattering expansion contained in the $qq \to qq$ subscattering process for proton-proton scattering. (a) quark+quark → quark+quark (quark recoil contribution). (b) diquark+gluon → quark+quark.

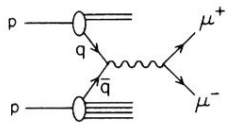

(a)

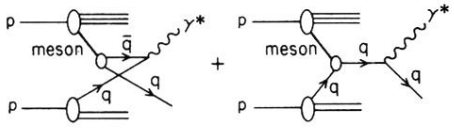

(b)

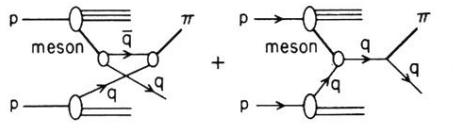

(c)

FIG. 11. (a) Drell-Yan subscatter $q\bar{q} \rightarrow \mu^+\mu^-$. (b) CIM subscatter $Mq \rightarrow \gamma^*(\rightarrow \mu^+\mu^-)q$. (c) CIM subscatter $Mq \rightarrow \pi q$.

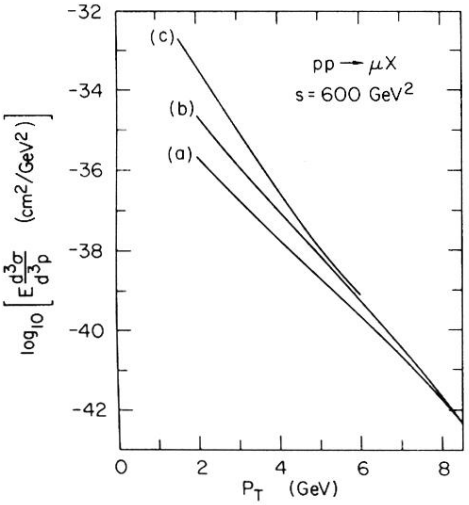

FIG. 12. $Ed^3\sigma/dp^3$ for single-μ production at high p_T for $s = 600$ GeV^2 (a) Drell-Yan, $q\bar{q} \to \mu^+ \mu^-$. (b) CIM, $Mq \to (\mu^+ \mu^-)q$. (c) Data (Ref. 23).

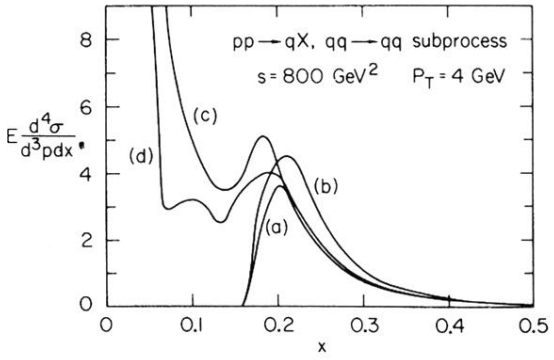

FIG. 13. $E(d^4\sigma/dp^3dx)$ versus x for quark-jet production ($qq \to qq$) for $s = 800$ GeV^2 and $p_T = 4$ GeV where x is the light-cone variable of one constituent. The normalization is arbitrary. The curves shown are (a) Cases (1) and (2) (given in Sec. IV D) for either on-shell or off-shell kinematics (these all coincide at this scale). (b) Off-shell kinematics with normalized e^{-3k_T} distribution (case 3). (c) On-shell kinematics with normalized e^{-3k_T} distribution (case 3) for $M_g = M_q$. (d) As (c) but for $M_g = \sqrt{10}\, M_q$.

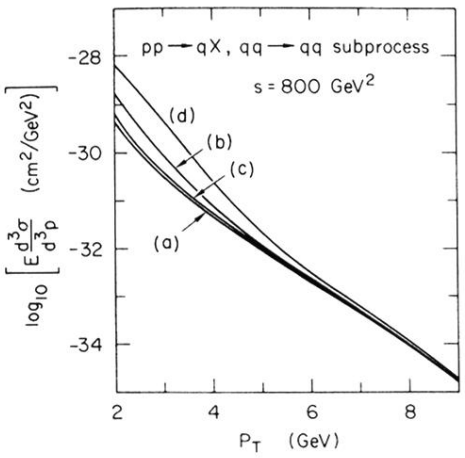

FIG. 14. $E(d^3\sigma/dp^3)$ for production of a quark jet at 90° versus p_T for $s = 800$ GeV^2. The curves shown are (a) As (a) in Fig. 13. (b) As (b) in Fig. 13. (c) Normalized $e^{-3k_T^2}$ distribution [case (4) Sec. IV D] for either on-shell or off-shell kinematics. (d) As (d) in Fig. 13.

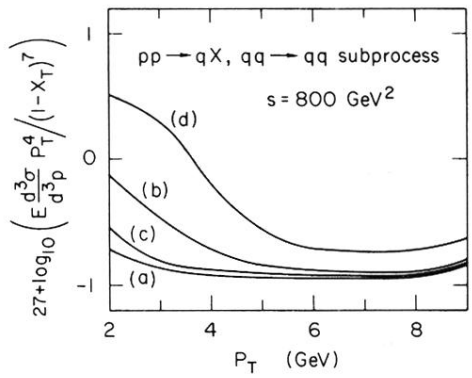

FIG. 15.

$$27+\log_{10}\left[E\frac{d^3\sigma}{dp^3}\,p_T{}^4/(1-x_T)^7\right]$$

for the cases (a)–(d) given in Fig. 14.

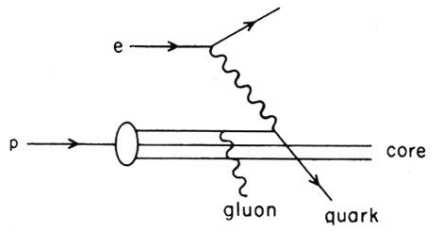

(a)

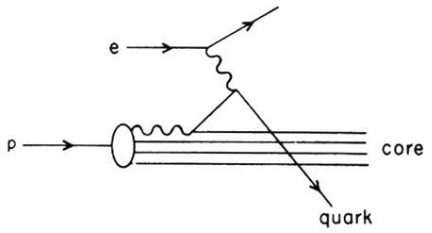

(b)

FIG. 16. Contributions to ep scattering from (a) $|qqqg\rangle$ wave functions and (b) $|qqqq\bar{q}\rangle$ wave functions.

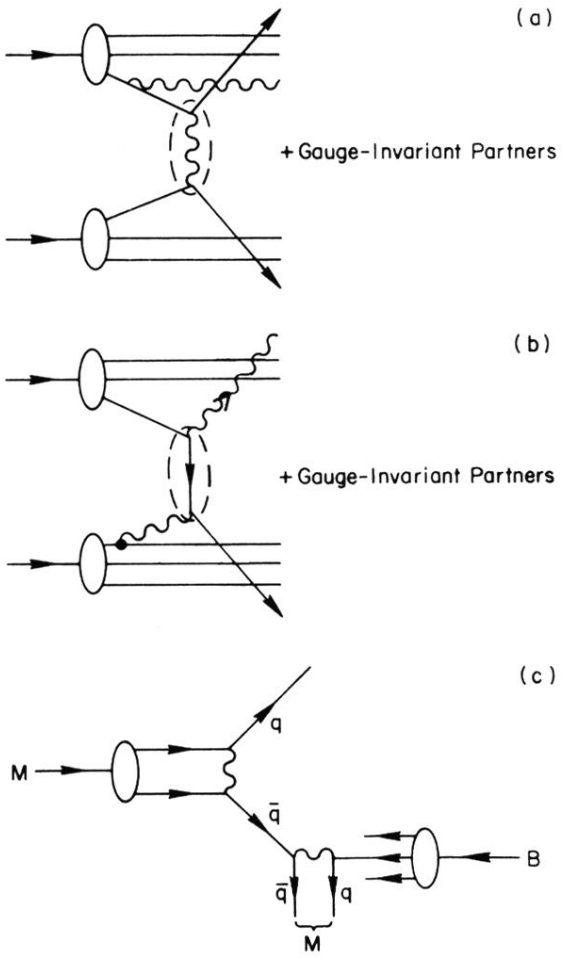

FIG. 2. (a) quark+quark→quark+quark (gluon brehmsstrahlung contribution). (b) quark+gluon→ gluon +quark. (c) The rearrangement of the $q\bar{q}\rightarrow q\bar{q}$ subscatter in $M+B$ scattering to show the contributing subprocess $M+q\rightarrow M+q$.

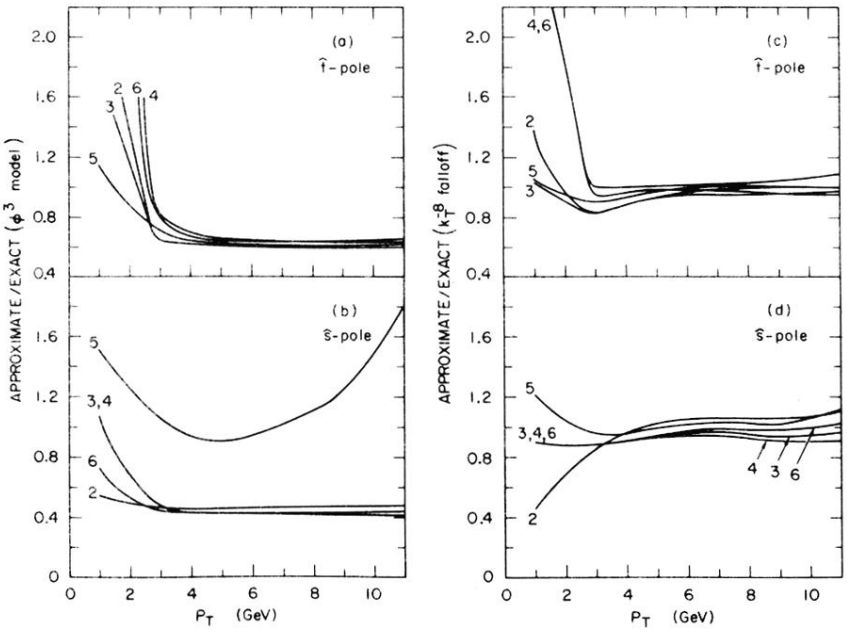

FIG. 3. The ratio of various approximate calculations to the exact calculation versus p_T ($s = 800$ GeV^2, $m = 1$ GeV) for high-p_T scattering in ϕ^3 field theory. The curves are labeled by the number of the particular approximation as given in Sec. II B. (a) $\hat{t}$-pole subprocess. (b) $\hat{s}$-pole subprocess. (c) $\hat{t}$-pole subprocess with (k_T^a, k_T^b) distribution replaced by $(k_T^2 + M(x^2)^{-4})$. The contribution of the subprocess of Fig. 1(d) is then suppressed. (d) As (c) but for $\hat{s}$-pole subprocess. The contributions of Fig. 1(e) and 1(f) are suppressed.

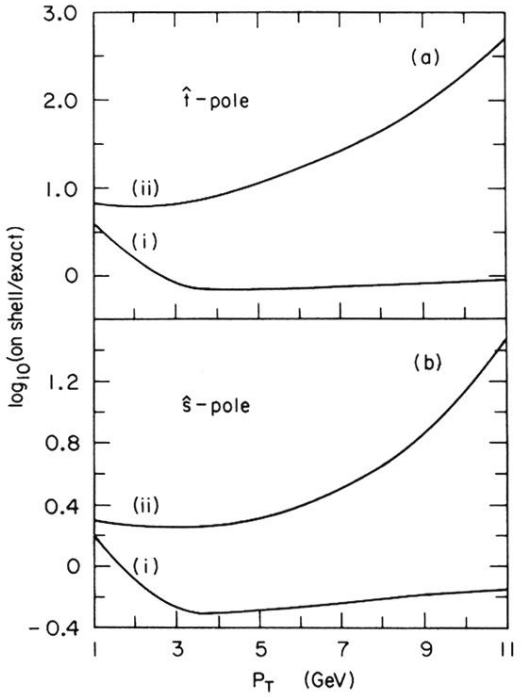

FIG. 4. Ratio of on-shell kinematics calculation to exact calculation versus p_T ($s = 800$ GeV^2, $m = 1$ GeV) for (i) no transverse fluctuations, (ii) $[k_T^2 + M(x)^2]^{-2}$ transverse-momentum distribution (logarithmic scale) (a) $\hat{t}$-pole subprocess. (b) $\hat{s}$-pole subprocess.

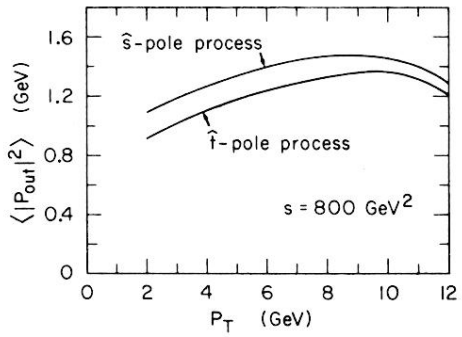

FIG. 5. $\langle |P_{\text{out}}|^2 \rangle$ distribution versus p_T ($s = 800$ GeV^2, $m = 1$ GeV) for (a) $\hat{t}$-pole subprocess (b) $\hat{s}$-pole subprocess.

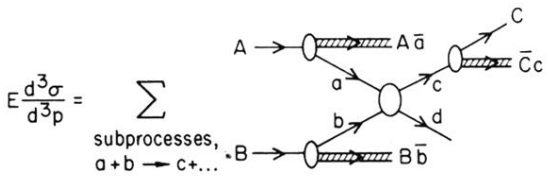

FIG. 6. Representation of hard-scattering expansion.

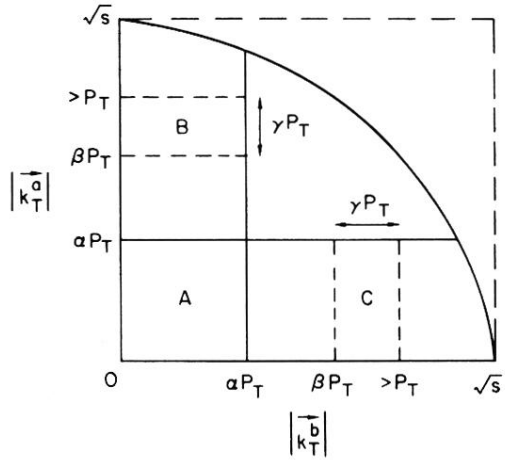

FIG. 7. A, B, C are the main areas of $(\vec{k}_a, \vec{k}_b)$ space contributing to the ϕ^3 field theory inclusive high-p_T scattering. $\alpha, \beta, \gamma \ll 1$, $\alpha p_T, \beta p_T, \gamma p_T \gg m_q$. These regions correspond to the different subprocesses shown in Fig. 1.

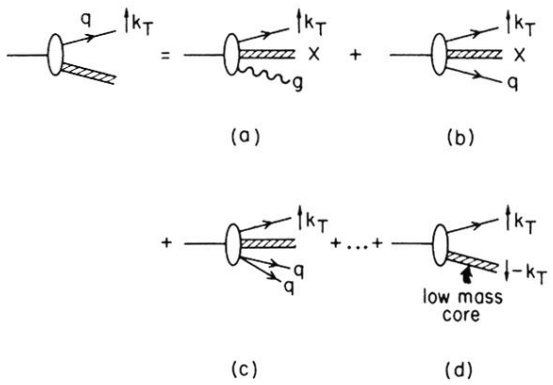

FIG. 8. The origin of quark transverse momentum in the hadron wave function showing the various recoil constituents and the remaining low-mass, low-k_T core X. See Eq. (4.1).

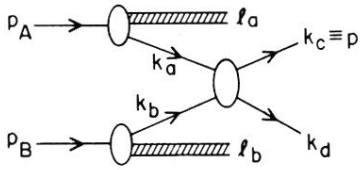

FIG. 9. Generic hadron + hadron → (high-p_T trigger) + X.